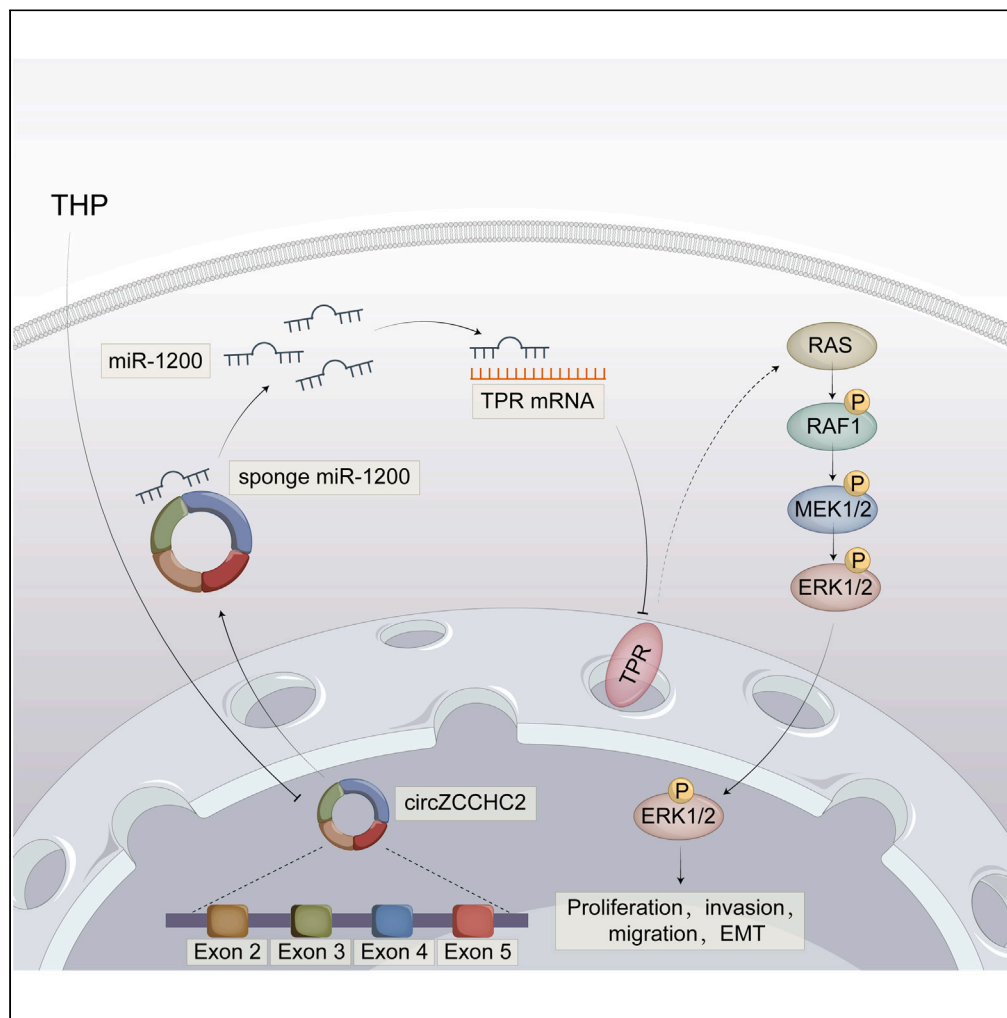


Article

CircZCCHC2 decreases pirarubicin sensitivity and promotes triple-negative breast cancer development via the miR-1200/TPR axis



Fan Zhang, Dexian Wei, Shishun Xie, ..., Liying Li, Jiahua Ji, Zhimin Fan

fanzm@jlu.edu.cn

Highlights

CircZCCHC2 promotes the proliferation, migration, invasion, and EMT of TNBC

CircZCCHC2 promotes TNBC progression via the miR-1200/TPR axis

CircZCCHC2 knockdown inhibited tumor growth *in vivo*

CircZCCHC2 decreases the sensitivity of TNBC cells to pirarubicin

Zhang et al., iScience 27, 109057
March 15, 2024 © 2024 The Author(s).
<https://doi.org/10.1016/j.isci.2024.109057>



Article

CircZCCHC2 decreases pirarubicin sensitivity and promotes triple-negative breast cancer development via the miR-1200/TPR axis

Fan Zhang,¹ Dexian Wei,² Shishun Xie,² Liqun Ren,² Sennan Qiao,² Liying Li,¹ Jiahua Ji,² and Zhimin Fan^{1,3,*}

SUMMARY

Triple-negative breast cancer (TNBC) has attracted attention due to its poor prognosis and limited treatment options. The mechanisms underlying the association between circular RNAs (circRNAs) and the occurrence and development of TNBC remain unclear. CircZCCHC2 is observed to be upregulated in TNBC cells, tissues, and plasma exosomes. Knockdown of circZCCHC2 inhibited the proliferation, migration, invasion, and epithelial-mesenchymal transition of TNBC cells *in vitro* and *in vivo*. Pirarubicin (THP) treatment downregulated circZCCHC2, and circZCCHC2 affected the sensitivity to THP. CircZCCHC2/miR-1200/translocated promoter region, the nuclear basket protein (TPR) pathway was cascaded and verified. It is demonstrated that circZCCHC2 plays a crucial role in the malignant progression of TNBC via the miR-1200/TPR axis, thereby activating the RAS-RAF-MEK-ERK pathway. The present results indicate that circZCCHC2 has the potential to serve as a novel prognostic biomarker for TNBC.

INTRODUCTION

According to the global cancer statistics for 2020, breast cancer (BC) has the highest incidence and mortality of all cancers in women.¹ Triple-negative breast cancer (TNBC) is characterized by negative estrogen receptor (ER), progesterone receptor (PR), and human epidermal growth factor receptor 2 (HER2) expression, and thus lacks treatment targets. The clinical treatment of TNBC consists mainly of surgery, radiation, and chemotherapy. Drug resistance and the lack of targeted treatments in TNBC have attracted research attention. Additionally, TNBC shows high levels of malignancy, invasiveness, and a high likelihood of recurrence and metastasis.^{2,3} Although the prognosis of TNBC has improved considerably, it remains an important problem.

Recent advances in high-throughput RNA-sequencing technology and bioinformatics tools have led to the identification of an increasing number of circular RNAs (circRNAs), which are distinguished by their closed-loop structure without a 5'-cap or a 3'-polyadenylated tail. CircRNAs can act as oncogenes or tumor suppressor genes and are strongly linked to the development and metastasis of BC^{4–7} and other types of tumors.^{8–10} CircRNAs can act by sponging microRNAs (miRNAs),¹¹ encoding proteins,^{12,13} and regulating parental genes.^{14–16} CircZCCHC2, a 374 bp-long-circRNA derived from exons 2–5 of the ZCCHC2 transcript (chr18: 60206913–60217693), has previously been reported to be associated with hepatocellular carcinoma,¹⁷ while its potential role in BC has not been investigated to date.

Exosomes are released into extracellular spaces by various cells and have a spherical bilayer vesicle structure with a diameter of 30–150 nm.¹⁸ Exosomes contain many mediators that can transmit signals between cells, such as circRNAs, long non-coding RNAs (lncRNAs), miRNAs, mRNA, DNA, proteins, and lipids.¹⁹ CircRNAs in exosomes are related to tumor proliferation,^{19–23} prognosis,²⁴ and drug resistance,²⁵ and have the potential to be used as tumor markers.²⁶

In this study, we identified circZCCHC2 through bioinformatics analysis and verified its upregulation in TNBC cells, tissues, and exosomes. We demonstrated that circZCCHC2 promotes TNBC proliferation, migration, invasion, and epithelial-mesenchymal transition (EMT) *in vitro* via the miR-1200/TPR (translocated promoter region, nuclear basket protein) axis and by activating the RAS-RAF-MEK-ERK pathway. We also found that pirarubicin (THP) plays a role in the treatment of BC by decreasing the expression of circZCCHC2. The role of circZCCHC2 in BC and pirarubicin resistance was confirmed *in vivo* in a xenograft tumor model. The findings of this study indicate that circZCCHC2 may serve as a target for diagnosis, treatment, and prognosis prediction in BC.

¹Department of Breast Surgery, General Surgery Center, The First Hospital of Jilin University, Changchun, Jilin 130021, China

²Department of Experimental Pharmacology and Toxicology, School of Pharmaceutical Sciences, Jilin University, 1266 Fujin Road, Changchun, Jilin 130021, China

³Lead contact

*Correspondence: fanzm@jlu.edu.cn

<https://doi.org/10.1016/j.isci.2024.109057>



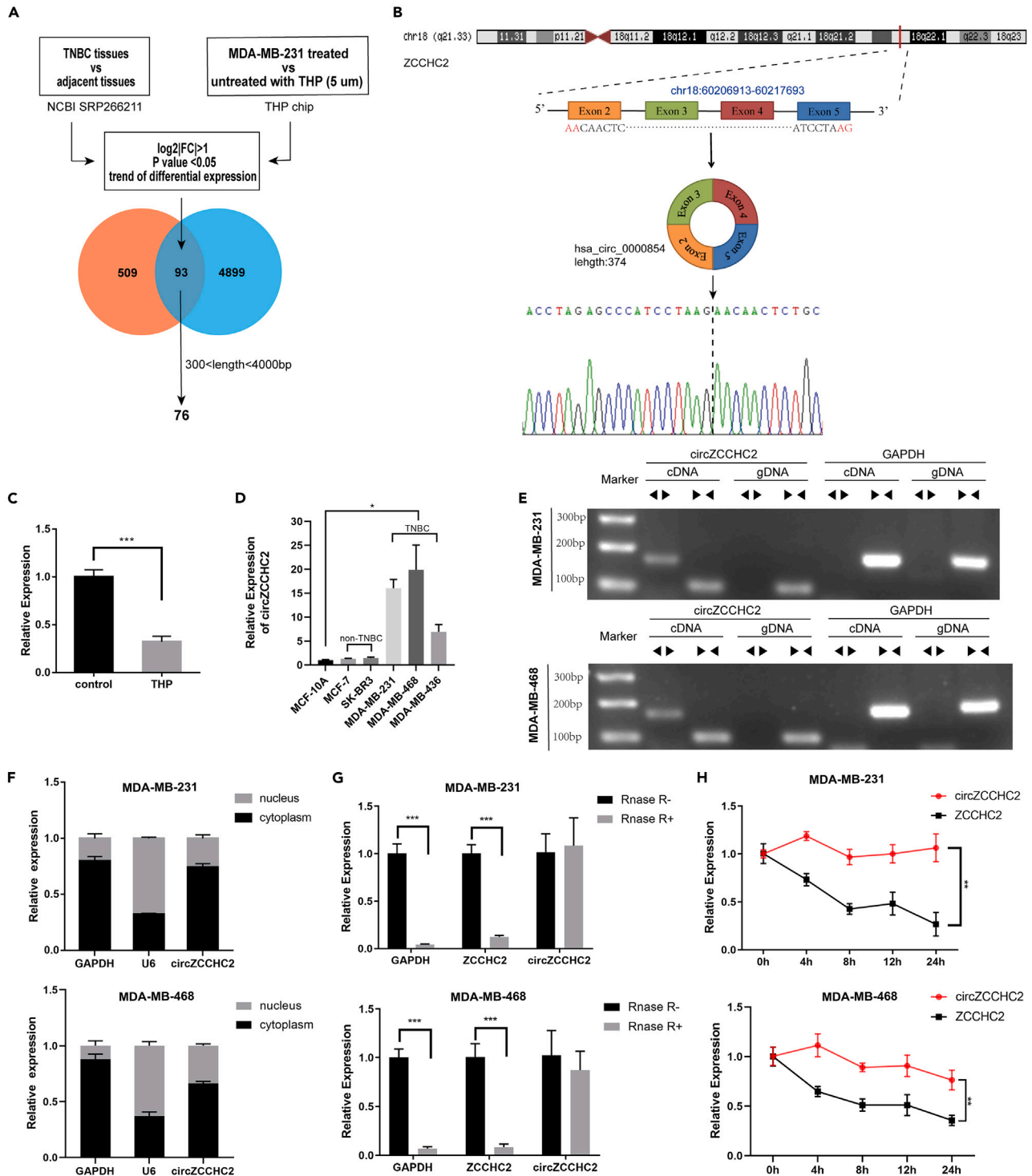


Figure 1. Expression and characterization of circZCCHC2 in TNBC cells

(A) Venn diagram illustrating the intersection of differentially expressed circRNAs in the NCBI SRP266211 dataset and gene chip data of MDA-MB-231 cells treated with THP (5 μ M) for 24 h.

(B) Schematic diagram of genomic information of circZCCHC2 (hsa_circ_0000854). The maternal gene location and exon composition are shown. The back-splicing site was identified by Sanger sequencing.

(C and D) RT-qPCR analysis of the relative expression levels of circZCCHC2 in MDA-MB-231 cells treated with and without THP (C), as well as normal breast epithelial cells and various types of breast cancer cells (D).

Figure 1. Continued

(E) Divergent and convergent primers were used to amplify reverse splicing and linear products to verify the presence of circZCCHC2.

(F) RT-qPCR analysis of the expression levels of GAPDH, U6, and circZCCHC2 in isolated cytoplasmic and nuclear fractions.

(G) Abundance of circZCCHC2, linear ZCCHC2, and GAPDH in TNBC cells determined by RT-qPCR after treatment with RNase R.

(H) The expression of circZCCHC2 and linear ZCCHC2 in TNBC cells treated with ActD was analyzed by RT-qPCR. Data are presented as the mean \pm SD (three independent experiments). * $p < 0.05$, ** $p < 0.01$, and *** $p < 0.001$.

RESULTS**CircZCCHC2 is overexpressed in TNBC**

The results of RNA high-throughput sequencing of five TNBC and paired normal tissue samples (NCBI SRP266211)²⁷ and a THP treatment chip (MDA-MB-231 cells treated with and without 5 μ M THP)²⁸ were analyzed to identify a circRNA relevant to both TNBC and THP treatment. The filter conditions were $\log_2|FC| > 1$ and $p < 0.05$. Considering the circular characteristics of circRNAs, we selected circRNAs of 300–4000 bp capable of forming a ring for subsequent screening and verification. We identified 76 candidate circRNAs (Figure 1A). Because of the therapeutic effect of THP on BC, we expected the expression trend of circRNAs to be reversed in the two chips. In the THP chip, hsa_circ_0000854 showed the most significant downward trend and was thus selected for further research. Hsa_circ_0000854 was named “circZCCHC2” because it is derived from exons 2–5 of the ZCCHC2 transcript (chr18: 60206913–60217693); it is 374 bp long and is located at the 18q21.33 amplicon (Figure 1B). RT-qPCR was performed to verify the results of both chips. CircZCCHC2 was markedly downregulated in MDA-MB-231 cells treated with THP (5 μ M, 24 h) compared with untreated cells (Figure 1C). As shown in Figure 1D, the expression of circZCCHC2 was higher in TNBC cells (MDA-MB-231, MDA-MB-468, and MDA-MB-436) than in non-TNBC cell lines (MCF-7 and SK-BR-3) and normal mammary epithelial cells (MCF-10A).

To verify the circular structure of circZCCHC2, we designed primers that target circZCCHC2 across the back-splicing site and analyzed the RT-qPCR products by Sanger sequencing. The results showed that the base sequence of the products obtained using the indicated primers was consistent with that of circZCCHC2 and crossed the back-splicing site (Figure 1B). Next, we performed RT-qPCR using the divergent and convergent primers of circZCCHC2 and GAPDH for cDNA and gDNA, respectively, and the amplified band results were examined by agarose electrophoresis. The results showed that the circular RNA circZCCHC2 could only be produced by cDNA instead of gDNA, whereas the linear RNAs were produced by both cDNA and gDNA (Figure 1E). The results of nucleoplasmic separation experiments indicated that circZCCHC2 was mainly expressed in the cytoplasm, providing a basis for subsequent experiments exploring the competitive endogenous RNA (ceRNA) mechanism (Figure 1F). Another characteristic of circular RNAs is that they are more stable than linear RNAs, which was verified by RNase R digestion and actinomycin D assays (Figures 1G and 1H).

CircZCCHC2 expression was detected in tumor tissues and adjacent tissues of 34 patients with TNBC and 24 patients with non-TNBC by RT-qPCR. CircZCCHC2 expression was significantly upregulated in tumor tissues from TNBC patients (Figure 2A, $p < 0.001$) and it was higher in TNBC than in non-TNBC tumor tissues (Figure 2A, $p < 0.001$). As shown in Figure 2B, the area under the curve (AUC) of circZCCHC2 was 0.787 ($p < 0.0001$), indicating that circZCCHC2 could distinguish BC from adjacent normal tissue. The cut-off value was at 0.471, the sensitivity was 0.765, and the specificity was 0.706 at the cut-off value. According to the median expression level of circZCCHC2, the 34 TNBC patients were divided into high and low expression groups. Analysis of the relationship between circZCCHC2 expression and clinicopathological characteristics showed that patients with high-circZCCHC2 expression had a higher risk of developing lymph node metastasis (Table 1, $p = 0.026$) and vascular infiltration (Table 1, $p = 0.044$). Next, we analyzed the correlation between plasma exosomal circZCCHC2 expression and BC. Transmission electron microscopy (TEM), a Malvern particle size meter, and western blotting were used to assess the characteristics of plasma exosomes (Figures 2C–2E). Plasma exosomes were extracted from 42 TNBC patients and 35 non-TNBC patients, and the expression of circZCCHC2 was analyzed by RT-qPCR. The results showed that circZCCHC2 expression was significantly higher in plasma exosomes of TNBC patients than in those of non-TNBC patients, confirming the triple-negative specificity of circZCCHC2 (Figure 2F). Correlation analysis of TNBC patients with high and low circZCCHC2 expression showed that the expression of circZCCHC2 in plasma exosomes was correlated with tumor size (Table 2, $p = 0.013$).

CircZCCHC2 promotes TNBC cell proliferation, migration, invasion and EMT

The RT-qPCR results showed that transfection with oe-circZCCHC2 significantly upregulated circZCCHC2 expression in MDA-MB-231 (Figure 3A) and MDA-MB-468 cells (Figure S1A), whereas sh-circZCCHC2 plasmid lentivirus downregulated circZCCHC2 expression. The results of the CCK-8 assay showed that downregulation of circZCCHC2 decreased, whereas its upregulation increased the proliferation ability of MDA-MB-231 (Figure 3B) and MDA-MB-468 cells (Figure S1B). The EdU assay demonstrated that knockdown of circZCCHC2 decreased the proportion of EdU-positive cells in both MDA-MB-231 and MDA-MB-468 cells, whereas overexpression had the opposite effect (Figures 3C and S1C). The wound-healing and Transwell assays showed that knockdown of circZCCHC2 significantly decreased the migration and invasion abilities of MDA-MB-231 and MDA-MB-468 cells, whereas overexpression had the opposite effects (Figures 3D, 3E, S1D, and S1E). Western blot analysis showed that downregulation of circZCCHC2 significantly decreased N-cadherin and vimentin expression and increased E-cadherin expression, whereas circZCCHC2 overexpression had the opposite effects (Figures 3F and S1F). Taken together, the results indicated that circZCCHC2 promotes cell proliferation, migration, invasion, and EMT.

MiR-1200 is a target of circZCCHC2, and circZCCHC2 regulates malignant progression by sponging miR-1200 in TNBC cells

The results of the nucleoplasmic separation experiments indicated that circZCCHC2 was mainly present in the TNBC cytoplasm; therefore, we hypothesized that circZCCHC2 might play a role in promoting malignant progression in TNBC through a ceRNA mechanism. Analysis of the

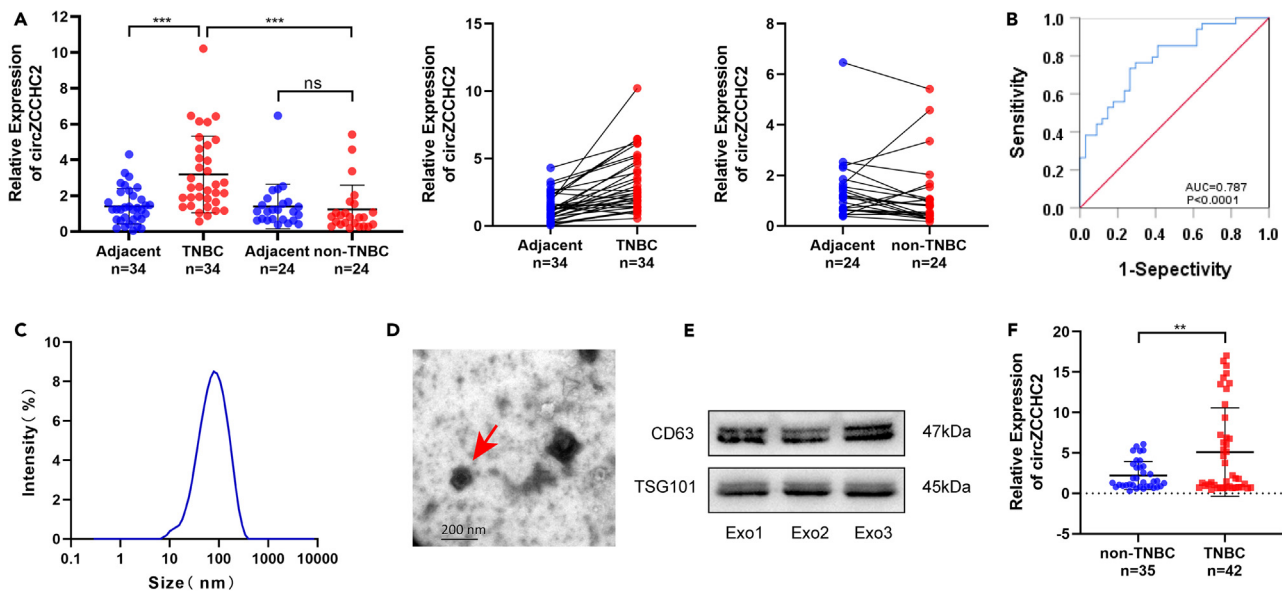


Figure 2. CircZCCHC2 is upregulated in TNBC tissues and plasma

(A) RT-qPCR analysis of the expression of circZCCHC2 in TNBC tissues, non-TNBC tissues, and their respective paired adjacent normal tissues. (B) ROC curve analysis demonstrated that the AUC of circZCCHC2 was 0.787 ($p < 0.0001$). The cut-off value was at 0.471, the sensitivity was 0.765, and the specificity was 0.706 at the cut-off value. (C–E) Plasma exosomes were identified by Malvern particle size meter (C), TEM (D), and western blotting (E). (F) RT-qPCR analysis of the expression of circZCCHC2 in the plasma exosomes of TNBC and non-TNBC patients. Data are presented as the mean \pm SD (three independent experiments). ** $p < 0.01$, *** $p < 0.001$, and ns: not significant.

circInteractome and circBank databases to predict miRNAs potentially targeting circZCCHC2 identified four candidate miRNAs (Figure 4A). The predicted binding sites of these four miRNAs with circZCCHC2 are shown in Figure 4B. Next, we performed RT-qPCR to determine the expression of the four candidate miRNAs in cells with circZCCHC2 overexpression and knockdown. We identified miR-1200 as the only miRNA upregulated by circZCCHC2 knockdown and downregulated by circZCCHC2 overexpression (Figure 4C). The specific binding site between circZCCHC2 and miR-1200 was identified using the circInteractome dataset (Figure 4D). Luciferase reporter assays (Figure 4E) to confirm binding between circZCCHC2 and miR-1200 showed that treatment of circZCCHC2 wild-type cells with miR-1200 mimics and inhibitor significantly decreased and increased luciferase reporter activity, respectively. By contrast, the circZCCHC2 mutant group showed no significant changes (Figure 4E). The results of the pull-down assay showed that circZCCHC2 was significantly pulled down by the biotin-labeled miR-1200 probe but not by the control probe (Figure 4F). Collectively, these findings indicated that circZCCHC2 binds directly to miR-1200. Pearson's correlation analysis showed a negative correlation between miR-1200 expression and circZCCHC2 (Figure 4G).

To determine whether circZCCHC2 enhanced the malignant progression of TNBC through miR-1200, rescue experiments were performed by treating circZCCHC2 knockdown TNBC cell lines with a miR-1200 inhibitor. CCK-8 and EdU assays showed that circZCCHC2 knockdown decreased TNBC cell proliferation, which was restored by miR-1200 inhibitor treatment (Figures 4H, 4I, S2A, and S2B). Wound-healing, Transwell, and western blot assays demonstrated that circZCCHC2 knockdown significantly decreased the migration, invasion, and EMT abilities of TNBC cells, whereas treatment with a miR-1200 inhibitor restored these effects (Figures 4J–4L and S2C–S2E). These findings confirmed that circZCCHC2 promoted the malignant progression of TNBC cells via miR-1200.

TPR is the direct target of miR-1200, and circZCCHC2 regulates TPR expression through miR-1200

To further examine the ceRNA mechanism, TargetScan and miRDB were used to predict the potential target downstream genes of miR-1200. After combining these data with the THP chip results, 315 candidate mRNAs were identified (Figure 5A). The Gene Ontology (GO) and Kyoto Encyclopedia of Genes and Genomes (KEGG) pathway enrichment tools were used to analyze the target genes (Figures 5B and 5C). KEGG analysis showed that miR-1200 was significantly correlated with 14 target mRNAs enriched in pathways in cancer (Figure 5D). Next, we performed RT-qPCR to determine the expression of the 14 candidate mRNAs in cells treated with miR-1200 mimics and inhibitor. The results showed that TPR was the most upregulated target mRNA when miR-1200 inhibitor was used, and it was also significantly downregulated with the treatment of miR-1200 mimics (Figure 5E). Thus, we identified TPR for further study. TPR was detected to be downregulated by circZCCHC2 knockdown and up-regulation by circZCCHC2 overexpression (Figure 5F). Furthermore, the downregulation of TPR caused by circZCCHC2 knockdown could be reversed by the miR-1200 inhibition (Figure 5G). The specific binding site between TPR and miR-1200 was analyzed using the TargetScan database (Figure 5H). The pull-down and luciferase reporter assays were performed to confirm binding between TPR and miR-1200. Treatment of TPR wild-type cells with miR-1200 mimics and inhibitor significantly decreased and increased

Table 1. Association between circZCCHC2 expression and clinicopathological features in triple-negative breast cancer tissue

| Variables | Cases | circZCCHC2 expression | | p value |
|-----------------------|-------|-----------------------|---------------|--------------|
| | | Low (n = 17) | High (n = 17) | |
| Age | | | | 0.491 |
| ≤50 | 15 | 6 | 9 | |
| >50 | 19 | 11 | 8 | |
| Tumor size (cm) | | | | 0.728 |
| ≤2 | 14 | 8 | 6 | |
| >2 | 20 | 9 | 11 | |
| Lymph node metastasis | | | | 0.026 |
| Negative | 23 | 15 | 8 | |
| Positive | 11 | 2 | 9 | |
| pTNM | | | | 0.398 |
| I-IIA | 27 | 15 | 12 | |
| IIB-III | 7 | 2 | 5 | |
| Vascular infiltration | | | | 0.044 |
| Negative | 29 | 17 | 12 | |
| Positive | 5 | 0 | 5 | |
| Ki-67 | | | | 0.656 |
| ≤30% | 6 | 2 | 4 | |
| >30% | 28 | 15 | 13 | |

The bold values represent a statistical difference ($p < 0.05$).

luciferase reporter activity, respectively. However, no changes were observed in the TPR mutant group (Figure 5J). The results of pull-down assays showed that TPR was significantly pulled down by the biotin-labeled miR-1200 probe but not by the control probe (Figure 5I). These results demonstrate that TPR directly binds to miR-1200, and circZCCHC2 regulates TPR expression through miR-1200. Pearson's correlation analysis showed that TPR expression was negatively correlated with miR-1200 and positively correlated with circZCCHC2 (Figure 5K).

miR-1200 regulates TPR to affect malignant progression of TNBC cells and may have effect on RAS-RAF-MEK-ERK signaling pathway

To further demonstrate that miR-1200 inhibits the malignant progression of TNBC cells via TPR, we performed rescue experiments using si-TPR transfection in TNBC cell lines treated with miR-1200 inhibitor. The CCK-8 and EdU assays showed that miR-1200 inhibitor transfection increased TNBC cell proliferation, and this effect was restored by si-TPR treatment (Figures 6A and 6B; S3A and S3B). The results of wound-healing, Transwell, and western blot assays demonstrated that miR-1200 inhibition significantly increased migration, invasion, and EMT in TNBC cells, and these effects were reversed by si-TPR treatment (Figures 6C–6E and S3C–S3E). KEGG pathway enrichment analysis suggested that TPR exerted its function via the RAS-RAF-MEK-ERK pathway. Western blot analysis showed that RAS, p-RAF1/RAF1, p-MEK1/2/MEK1/2, and p-ERK1/2/ERK1/2 were upregulated by treatment with miR-1200 inhibitor, and this upregulation was partially reversed by exposure to si-TPR (Figures 6F and S3F). Taken together, these results confirmed that knockdown of TPR partly reversed the effects of miR-1200 inhibition on malignant progression in TNBC cells.

THP inhibits the malignant progression of TNBC cells by downregulating circZCCHC2 expression

We further verified whether THP inhibits the malignant progression of TNBC cells by down-regulating circZCCHC2. CCK-8 assay showed that the IC₅₀ of THP on MDA-MB-231 and MDA-MB-468 were about 5 μM and 3 μM, respectively (Figures 7A and S4A). The results of RT-qPCR showed that treatment with THP (5 μM for MDA-MB-231 and 3 μM for MDA-MB-468) significantly downregulated circZCCHC2 expression in TNBC cells (Figures 7B and S4B). The CCK-8 and EdU assays demonstrated that THP effectively suppressed the proliferation of TNBC cells. Wound-healing, Transwell, and western blot assays demonstrated that THP suppressed the migration, invasion, and EMT abilities of TNBC cells, and downregulated RAS, p-RAF1/RAF1, p-MEK1/2/MEK1/2, and p-ERK1/2/ERK1/2. Overexpression of circZCCHC2 partially reversed the effect of THP on inhibiting malignant progression in TNBC cells (Figures 7C–7H and S4C–S4H).

Table 2. Association between circZCCHC2 expression and clinicopathological features in plasma exosomes of triple-negative breast cancer patients

| Variables | Cases | circZCCHC2 expression | | p value |
|-----------------------|-------|-----------------------|---------------|---------|
| | | Low (n = 21) | High (n = 21) | |
| Age | | | | 1 |
| ≤50 | 18 | 9 | 9 | |
| >50 | 24 | 12 | 12 | |
| Tumor size (cm) | | | | 0.013 |
| ≤2 | 18 | 13 | 5 | |
| >2 | 24 | 8 | 16 | |
| Lymph node metastasis | | | | 1 |
| Negative | 29 | 14 | 15 | |
| Positive | 13 | 7 | 6 | |
| pTNM | | | | 0.130 |
| I-IIA | 33 | 19 | 14 | |
| IIB-III | 9 | 2 | 7 | |
| Vascular infiltration | | | | 0.184 |
| Negative | 36 | 16 | 20 | |
| Positive | 6 | 5 | 1 | |
| Ki-67 | | | | 0.719 |
| ≤30% | 10 | 6 | 4 | |
| >30% | 32 | 15 | 17 | |

The bold values represent a statistical difference ($p < 0.05$).

CircZCCHC2 decreases the sensitivity of TNBC cells to THP

To evaluate the biological role of circZCCHC2 on THP sensitivity of TNBC, CCK-8 assay was used to detect the cell viability. It was indicated that after the treatment of THP in gradient concentrations, overexpressed circZCCHC2 and miR-1200 inhibition decreased the efficacy of THP and increased the IC50 values while circZCCHC2 knockdown, si-TPR, and U0126 significantly enhanced the efficacy of THP and decreased the IC50 values (Figures 8A–8D and S5A–S5D). The rescue experiments demonstrated that when we treated cells with THP (MDA-MB-231 with 5 μ M and MDA-MB-468 with 3 μ M), the decrease in cell viability caused by circZCCHC2 knockdown could be reversed by miR-1200 inhibition, while the increase in cell viability caused by miR-1200 inhibition and circZCCHC2 overexpression could be reversed by si-TPR and U0126, respectively (Figures 8E and S5E).

CircZCCHC2 accelerates xenograft tumor growth and reduces sensitivity to THP *in vivo*

The role of circZCCHC2 in the growth and THP sensitivity of MDA-MB-231 cells was examined *in vivo* using a xenograft tumor model. Tumors derived from MDA-MB-231 cells stably overexpressing circZCCHC2 were larger in size, whereas tumors derived from MDA-MB-231 cells transduced with lentiviral shRNA targeting circZCCHC2 were smaller than those in the negative control (NC) group (Figures 9A–9C). The tumor volume and weight of the con, OE-NC, and OE groups were significantly lower in mice treated with THP than in the untreated group. Comparison of the tumors from the OE + THP group with those in the OE-NC + THP group showed that circZCCHC2 overexpression partially rescued the tumor inhibitory effect of THP (Figures 9A–9C). Western blotting (Figures 9G and 9H) and RT-qPCR (Figures 9D–9F) results showed that tumors derived from MDA-MB-231 cells stably overexpressing circZCCHC2 showed increased expression of circZCCHC2, TPR, N-cadherin, vimentin, RAS, p-RAF1/RAF1, p-MEK1/2/MEK1/2, and p-ERK1/2/ERK1/2, whereas miR-1200 and E-cadherin were downregulated. By contrast, tumors in the sh-circZCCHC2 group showed the opposite pattern. The expression of circZCCHC2, TPR, N-cadherin, vimentin, RAS, p-RAF1/RAF1, p-MEK1/2/MEK1/2, and p-ERK1/2/ERK1/2 was significantly lower in the con+THP and OE-NC + THP groups, whereas the expression of miR-1200 and E-cadherin was significantly higher compared with the control and OE-NC groups. These trends were partially reversed in the OE + THP group compared with the OE-NC + THP group. These results indicated that circZCCHC2 promoted xenograft tumor growth and decreases the sensitivity to THP *in vivo*.

DISCUSSION

CircRNAs, which occur abundantly in eukaryotic cells, are formed by covalent closed connections between the downstream 5' splice donor site and the upstream 3' splice acceptor site.¹⁹ CircRNAs are more stable than linear RNAs and less susceptible to degradation by RNA exonucleases such as RNase R. CircRNAs are involved in the development of cancer and can be considered as possible cancer biomarkers and

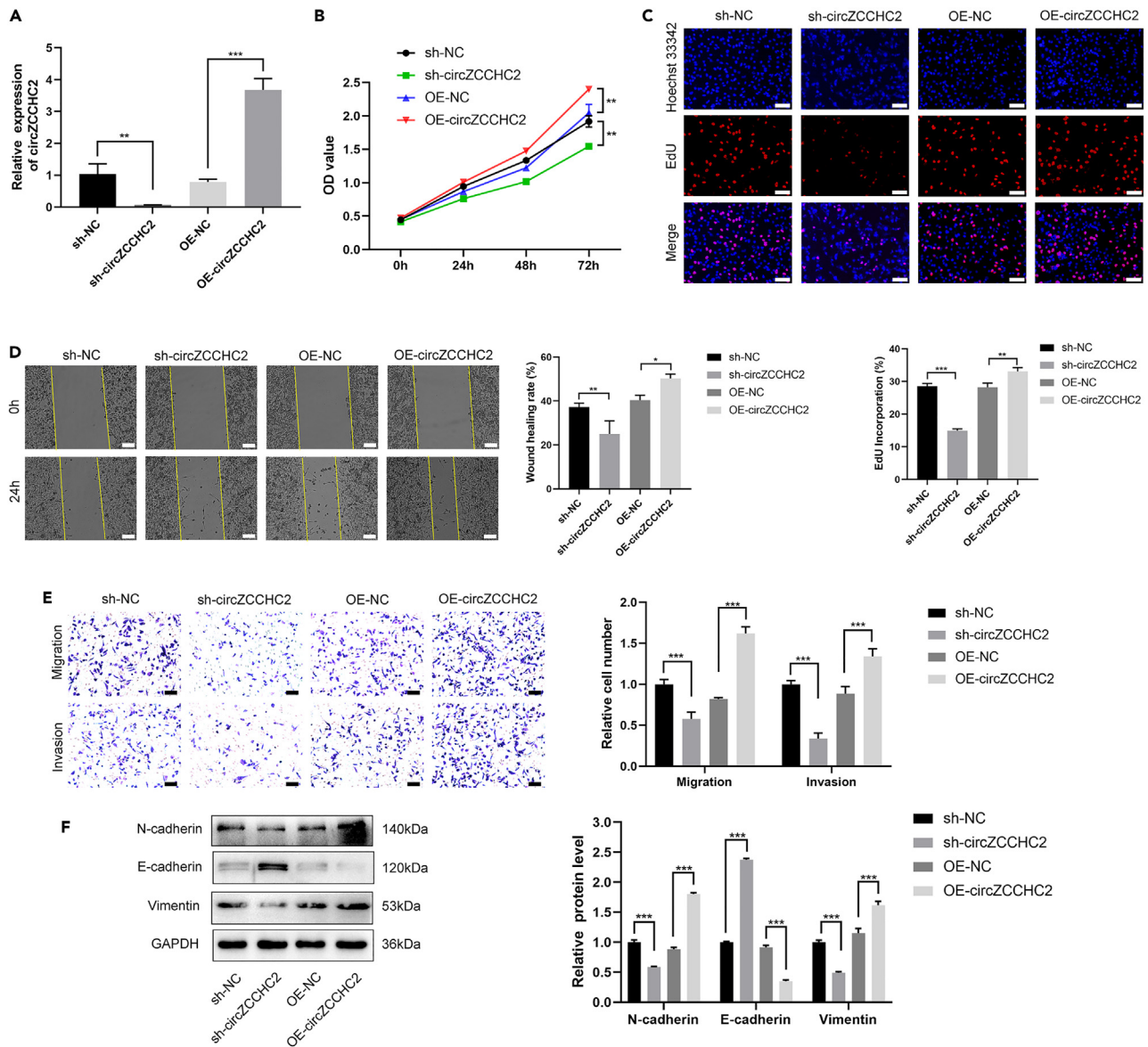


Figure 3. CircZCCHC2 promotes the proliferation, migration, invasion, and EMT of MDA-MB-231 cells *in vitro*

(A) RT-qPCR analysis of the expression of circZCCHC2 in MDA-MB-231 cells stably transfected with circZCCHC2 overexpression and knockdown vectors.

(B) The effect of circZCCHC2 on cell proliferation was evaluated using the CCK-8 assay.

(C) The effect of circZCCHC2 on cell proliferation was evaluated using the EdU assay (scale bar = 50 μ m).

(D) The wound-healing assay was used to evaluate the effect of circZCCHC2 on the migration ability of TNBC cells (scale bar = 100 μ m).

(E) The Transwell assay was used to evaluate the effect of circZCCHC2 on the migration and invasion abilities of TNBC cells (scale bar = 20 μ m).

(F) Western blotting was used to evaluate the effect of circZCCHC2 on EMT in MDA-MB-231 cells. Data are presented as the mean \pm SD (three independent experiments). * p < 0.05, ** p < 0.01, and *** p < 0.001.

therapeutic targets.^{29,30} Studies show that circRNAs are differentially expressed in TNBC cells and tissues.^{31,32} In this study, bioinformatics analysis and experimental data indicate that circZCCHC2 is upregulated in TNBC cells and tissues. In addition, many studies have also demonstrated the association between circRNAs and the occurrence, development, and pathophysiology of BC.^{33,34} Although the role of circZCCHC2 (hsa_circ_0000854) in regulating the malignant progression of hepatocellular carcinoma through the miR-1294/IRGQ axis has been demonstrated,¹⁷ its function and underlying mechanism in TNBC remain unclear. In this study, *in vivo* and *in vitro* experiments confirmed that circZCCHC2 promotes the malignant progression of TNBC by affecting cell proliferation, migration, invasion, and EMT, as well as the growth of xenograft tumors. Furthermore, the analysis of circZCCHC2 expression in the tumor tissues of BC patients demonstrated

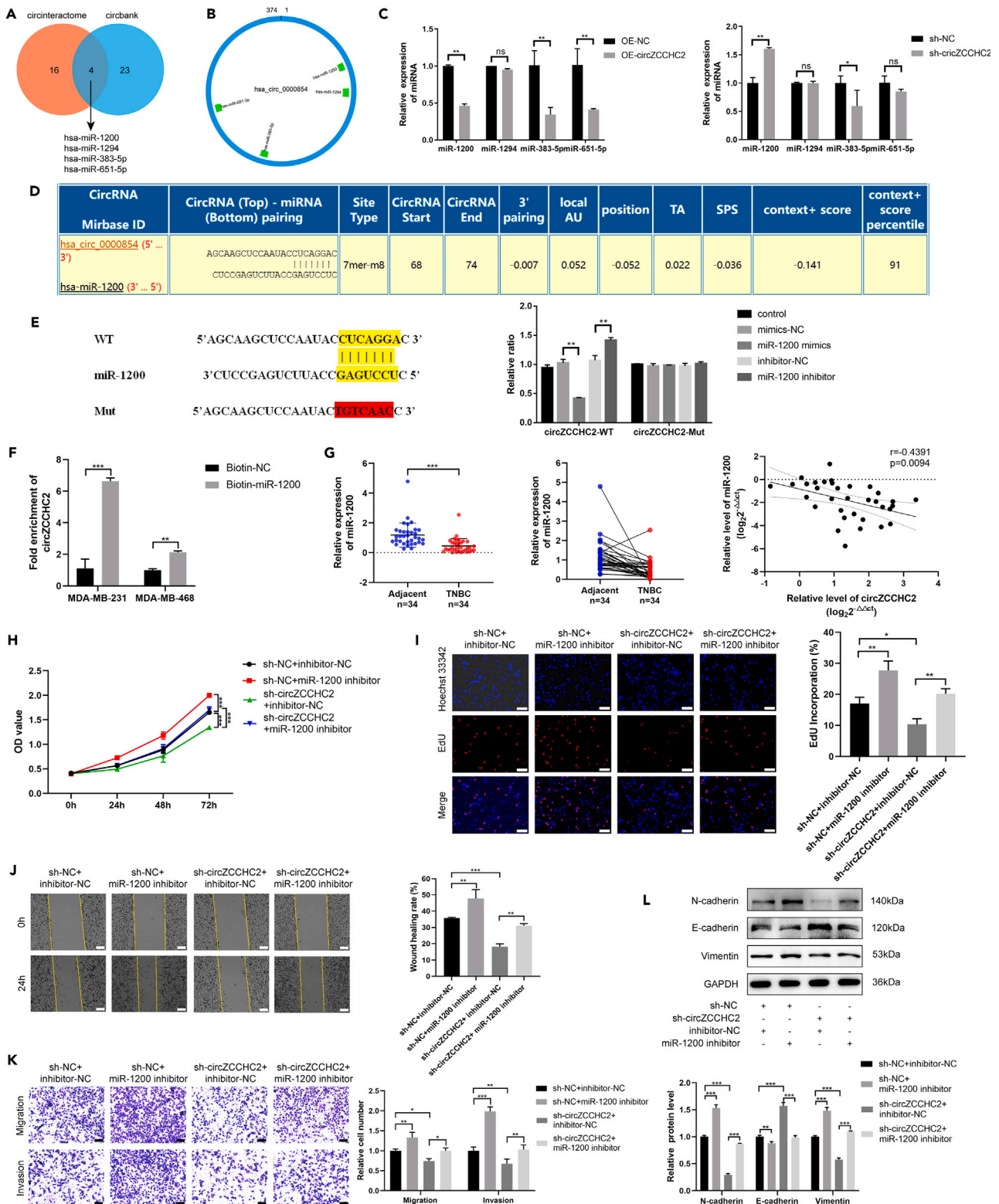


Figure 4. CircZCCHC2 acts as a miR-1200 sponge and promotes the malignant transformation of TNBC through miR-1200

(A) Venn diagram showing the intersection of potential target miRNAs of circZCCHC2 using circInteractome and circBank.
(B) Map of circZCCHC2 predicted miRNAs binding sites.

Figure 4. Continued

(C) RT-qPCR analysis showing the expression of four candidate miRNAs after circZCCHC2 overexpression and knockdown.

(D) The binding sites between circZCCHC2 and miR-1200 were predicted by circInteractome.

(E) A dual-luciferase reporter assay was used to detect luciferase activity after co-transfection with circZCCHC2-WT or circZCCHC2-MUT, and miR-NC or miR-1200.

(F) Pulldown assay of 3'-terminal biotinylated miR-1200 in TNBC cells followed by RT-qPCR to detect circZCCHC2 enrichment.

(G) RT-qPCR analysis of the expression of miR-1200 in TNBC tissues and the respective paired adjacent normal tissues (n = 34). The correlation between circZCCHC2 and miR-1200 expression in TNBC tissues was analyzed by Pearson's correlation analysis.

(H–L) MDA-MB-231 cells were transfected with a miR-1200 inhibitor and a sh-circZCCHC2 vector. The CCK-8 assay (H), EdU assay (I) (scale bar = 50 μ m), wound-healing assay (J) (scale bar = 100 μ m), Transwell assay (K) (scale bar = 20 μ m), and western blotting (L) were performed to analyze cell proliferation, migration, invasion, and EMT, respectively. Data are presented as the mean \pm SD (three independent experiments). *p < 0.05, **p < 0.01, ***p < 0.001, and ns: not significant.

correlations with important clinicopathological features including lymph node metastasis and vascular infiltration. In addition, circZCCHC2 expression in tumors compared with adjacent normal tissues suggested its potential as a diagnostic biomarker for BC.

CircRNAs can affect tumor formation and malignant progression through different mechanisms, such as acting as miRNA sponges, encoding proteins, and regulating parental genes. MiRNAs bind to target mRNAs through miRNA response elements (MREs) present on mRNA, thereby inhibiting mRNA translation or promoting its degradation, and thus regulating gene expression at the post-transcriptional level.³⁵ MREs exist not only on mRNA, but also on other types of RNA, such as circRNAs, suggesting that circRNAs can also bind to miRNAs and thus regulate miRNA expression.³⁶ The same miRNA can bind to multiple types of RNAs, and these different types of RNA molecules can compete with each other, which is known as the ceRNA mechanism. The ceRNA hypothesis has revealed a new mechanism of interaction between RNAs. MiRNAs can silence genes by binding to mRNA, whereas circRNAs can regulate the activity of miRNAs in modulating downstream RNA by competitively binding to miRNAs through MREs. This competitive binding of miRNAs is also known as miRNA sponging and has been widely reported in BC-related studies.^{6,37–41}

To examine the mechanism underlying the role of circZCCHC2 in TNBC, we first verified the localization of circZCCHC2 within the cell. Because circZCCHC2 is mainly located in the cytoplasm and circRNAs can target multiple miRNAs, we hypothesized that it may act through a ceRNA mechanism. We identified miR-1200 as target miRNA of circZCCHC2 through bioinformatics analysis. Dual luciferase assays verified the binding site between miR-1200 and circZCCHC2. Although miR-1200 is known to suppress the progression of tumors,^{26,42,43} whether miR-1200 is involved in TNBC and the underlying mechanisms remain unclear. The current research indicates, that miR-1200 acts as a tumor suppressor in TNBC. And reverse experiments indicated that circZCCHC2 promotes the malignancy of TNBC through miR-1200.

TPR is one of the building blocks of the nuclear pore complex.^{44,45} TPR proteins localize to the nuclear pore basket and are potential proto-oncogenic proteins (a protein that forms nuclear pores and is expressed abnormally in various cancers in the context of carcinogenic fusion with other proteins).⁴⁶ TPR plays a key role in mitosis through its transport to the spindle and centrosome and by binding to and interacting with the MAD1L1-MAD2L1 cell cycle checkpoint protein complex, aurora kinase A, and the dynein/dynein molecular motor complex.^{47,48} Some studies have shown that TPR is involved in the development and progression of cancers.^{46,49,50} However, there are few studies on the role of TPR in BC. The involvement of TPR was suggested in a study reporting that LINC01705 regulates BC progression through the miR-186-5p/TPR axis.⁵¹ In this study, we found that the expression of TPR was markedly upregulated in tumor tissues of TNBC patients compared with adjacent normal tissues and demonstrated the involvement of the circZCCHC2/miR-1200/TPR axis in TNBC.

The RAS/RAF/MEK/ERK pathway is a well-characterized MAPK pathway.⁵² It is a highly activated signaling pathway involved in the regulation of cell apoptosis, survival, metastasis, and invasion, and it plays crucial roles in cancer development and progression.^{53–55} This signaling pathway also provides research directions to investigate drug resistance and treatment options for BC. *Polygonatum odoratum* lectin was reported to induce MCF-7 cell apoptosis and autophagy by targeting EGFR-mediated RAS-RAF-MEK-ERK signaling pathway.⁵⁶ Combination therapy with miR34a and doxorubicin synergistically inhibits Dox-resistant BC progression by downregulating Snail through the suppression of the Notch/NF- κ B and RAS/RAF/MEK/ERK signaling pathways.⁵⁷ A novel hydrogen sulfide-releasing donor, HA-ADT, suppresses the growth of BC tumors by inhibiting the PI3K/AKT/mTOR and RAS/RAF/MEK/ERK signaling pathways.⁵⁸ It was reported that MEK-inhibitor E6201 could inhibit TNBC cells in a dose-dependent manner.⁵⁹ Copper chelation therapy could reduce the metastasis to the lung in the TNBC mouse model. At the same time, it could significantly reduce EMT by downregulating TGF- β /RAS/RAF/MEK/ERK and other pathways in cancer cells.⁶⁰ Enforcing mitochondrial fission inhibited migration, invasion, and metastasis in TNBC through PI3K/Akt/mTOR and Ras/Raf/MEK/ERK.⁶¹ In this study, we demonstrated the involvement of the RAS/RAF/MEK/ERK pathway in TNBC.

Exosomes are endosome-derived nanovesicles that contain materials from the host cell, such as proteins, lipids, DNA, and RNA.⁶² Exosomes are present in many body fluids, such as malignant effusions,⁶³ plasma,⁶⁴ urine,⁶⁵ and breast milk.⁶⁶ Their unique proteo-lipid architecture allows exosomes to cross various natural barriers and protects their cargo from degradation in the bloodstream.⁶⁷ These vesicles are secreted through exocytosis and taken up by other cells, thereby affecting their function and behavior, and they can be used as drug carriers for cancer treatment.^{68,69} CircRNAs in plasma exosomes of tumor patients can serve as non-invasive biomarkers for the early diagnosis, efficacy evaluation, and prediction of treatment outcome in cancer.^{70–73} The contribution of exo-circRNAs to BC progression was demonstrated previously. Endoplasmic reticulum stress stimulates BC cells to release exosomal circ_0001142 and induces M2 polarization of macrophages to regulate tumor progression through the circ_0001142/miR-361-3p/PIK3CB pathway.⁷⁴ Hsa_circ_0000615 is expressed at higher levels in the plasma of BC patients than in healthy controls, and the level of expression is associated with advanced tumor stage, lymph node

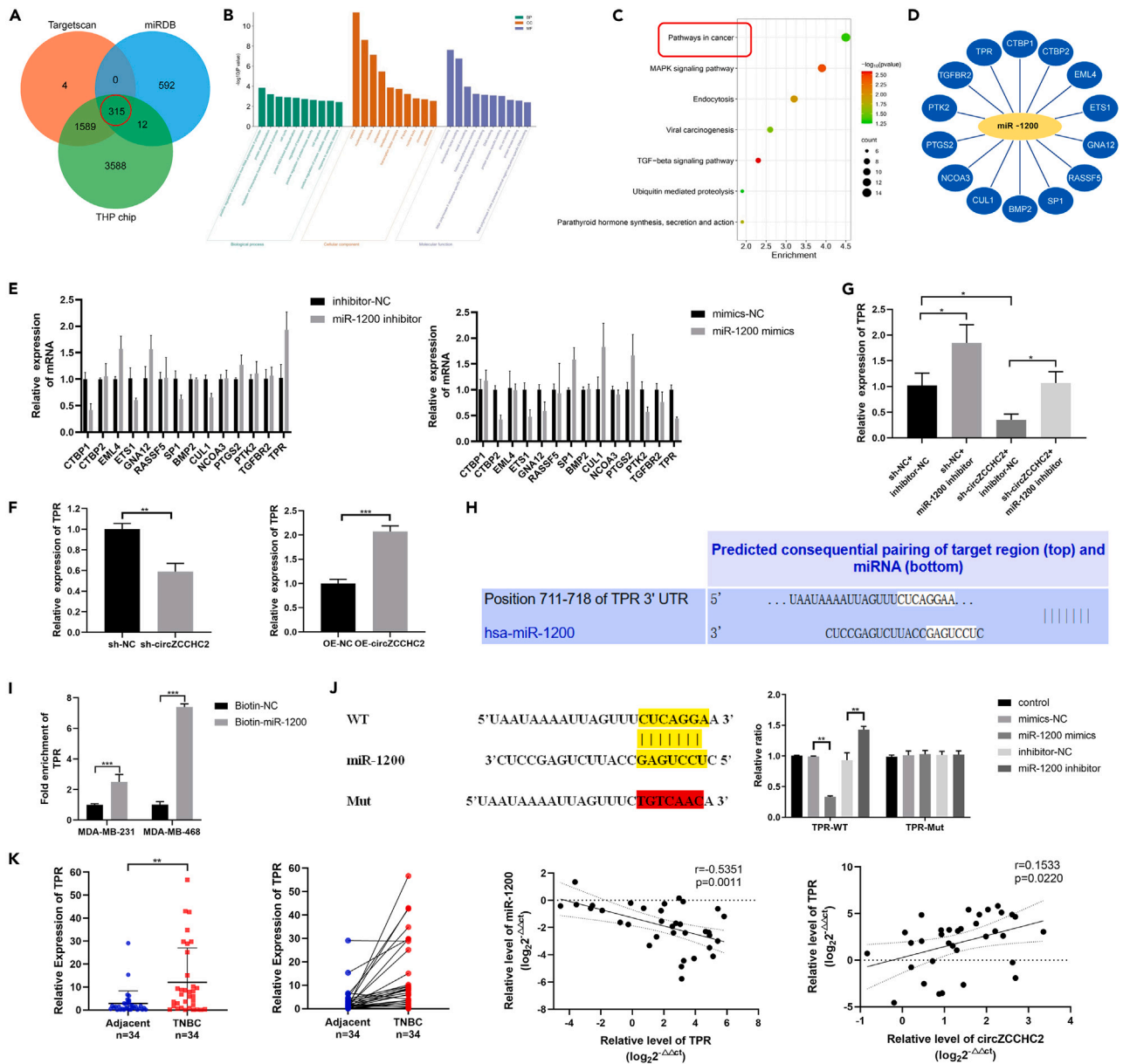


Figure 5. TPR is a direct target of miR-1200 in TNBC cells

(A) Venn diagram showing the intersection of potential target genes of miR-1200 using Targetscan, miRDB, and the gene chip data of MDA-MB-231 cells treated with THP (5 μ M) for 24 h.

(B and C) GO and KEGG analysis of the candidate genes.

(D) Candidate genes associated with pathways in cancer.

(E) RT-qPCR analysis of the expression of the 14 candidate genes after transfection with miR-1200 inhibitor and mimics.

(F) RT-qPCR analysis of the expression of TPR after circZCCHC2 overexpression and knockdown.

(G) TNBC cells were transfected with miR-1200 inhibitor and a circZCCHC2 knockdown vector followed by RT-qPCR to evaluate the expression of TPR.

(H) The binding sites of 3'-terminal biotinylated miR-1200 were predicted by TargetScan.

(I) A pull-down assay of 3'-terminal biotinylated miR-1200 was performed in TNBC cells, followed by RT-qPCR to detect TPR enrichment.

(J) A dual-luciferase reporter assay was used to detect luciferase activity after co-transfection with TPR-WT or TPR-MUT, and miR-NC or miR-1200.

(K) RT-qPCR was performed to evaluate the expression of TPR in TNBC tissues and the respective paired adjacent normal tissues (n = 34). The correlations between circZCCHC2, miR-1200, and TPR in TNBC tissues were analyzed by Pearson's correlation analysis. Data are presented as the mean \pm SD (three independent experiments). $*p < 0.05$, $**p < 0.01$, and $***p < 0.001$.

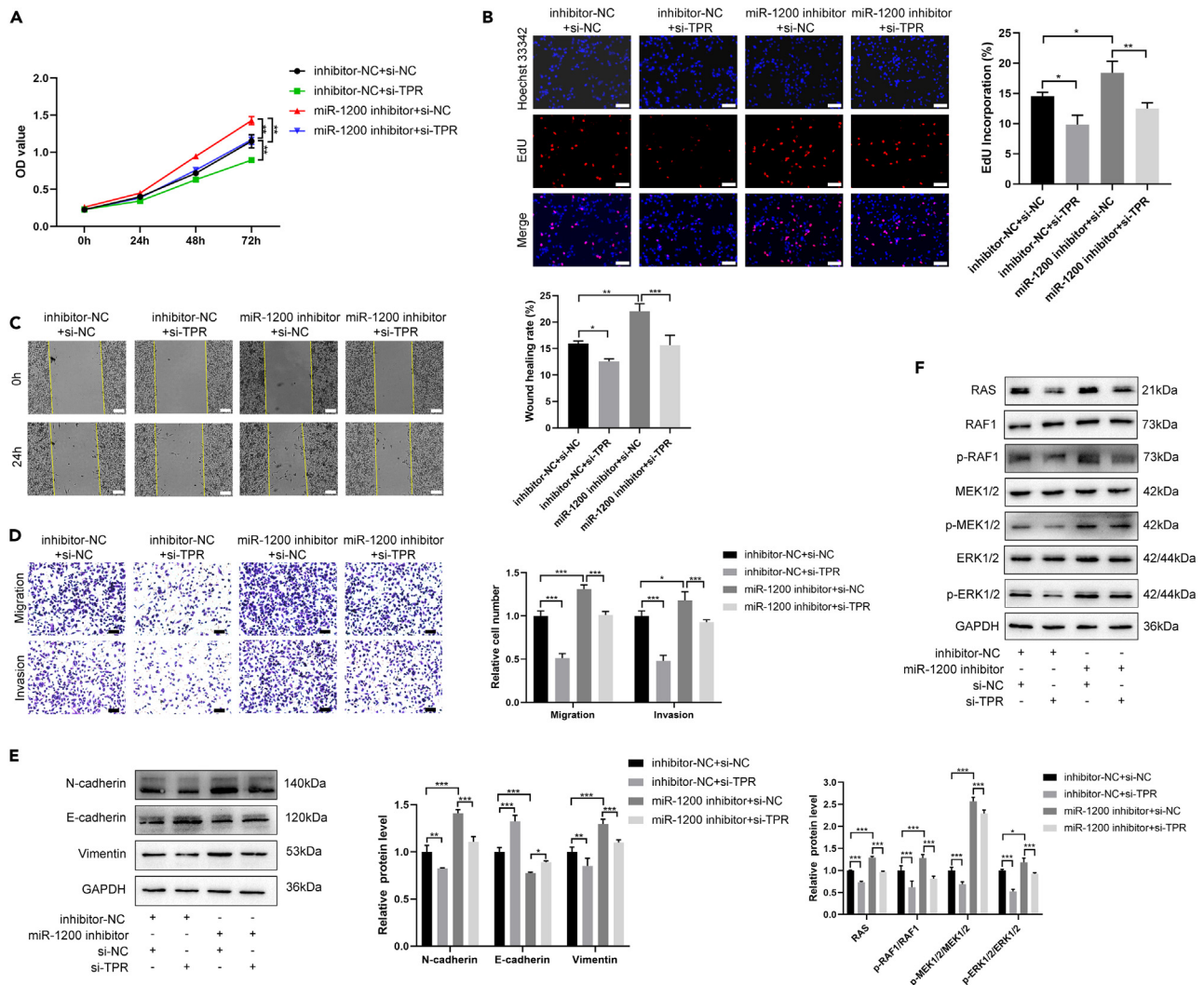


Figure 6. MiR-1200 promotes malignant transformation in TNBC through TPR

(A–F) MDA-MB-231 cells were transfected with miR-1200 inhibitor and si-TPR. The CCK-8 assay (A), EdU assay (B) (scale bar = 50 μ m), wound-healing assay (C) (scale bar = 100 μ m), Transwell assay (D) (scale bar = 20 μ m), and western blotting (E) were used to analyze cell proliferation, migration, invasion, and EMT, respectively. (F) The expression levels of RAS-RAF-MEK-ERK pathway effectors, including RAS, RAF1, p-RAF1, MEK1/2, p-MEK1/2, ERK1/2, and p-ERK1/2, were detected by western blotting. Data are presented as the mean \pm SD (three independent experiments). * p < 0.05, ** p < 0.01, and *** p < 0.001.

metastasis, and the risk of recurrence.⁷⁰ In this study, circZCCHC2 expression was significantly higher in plasma exosomes from TNBC patients than in non-TNBC patients, and high circZCCHC2 expression was associated with tumor size.

TNBC is characterized by negative expression of ER, PR, and HER2, and because of these molecular characteristics, the treatment of TNBC is challenging. Surgery, radiation, and chemotherapy remain the primary treatment methods for TNBC. In clinical practice, chemotherapy regimens based on anthracyclines and paclitaxel are the first choice of treatment. THP is a common anthracycline chemotherapy drug. It is generally believed that anthracycline inhibits DNA replication and RNA synthesis by embedding DNA double helix nucleic acid base pairs and inhibiting DNA topoisomerase II activity.^{75–78} In this study, we found and verified through the THP chip and RT-qPCR that the expression of circZCCHC2 in TNBC cells would decrease after the treatment of THP. However, the exact mechanism of this phenomenon is not clear. We hypothesized that THP may affect the expression of some splicing factors. Research found that hundreds of circRNAs were regulated in the process of EMT and more than one-third of the generation of circRNAs was dynamically regulated by the alternative splicing factor Quaking.⁷⁹ In addition, some transcription factors and post-transcriptional regulatory factors have also been reported to affect circRNA expression.^{80,81} CircRNA circSEPT9 was reported to be mediated by E2F1 and EIF4A3 in TNBC.³³ Additionally, doxorubicin was reported to induce RNA m6A methylation⁸² and some circRNAs were also reported to be modified by N6-Methyladenosine.⁸³ All these provide new research ideas for us to further explore the changes of circZCCHC2 expression caused by THP treatment.

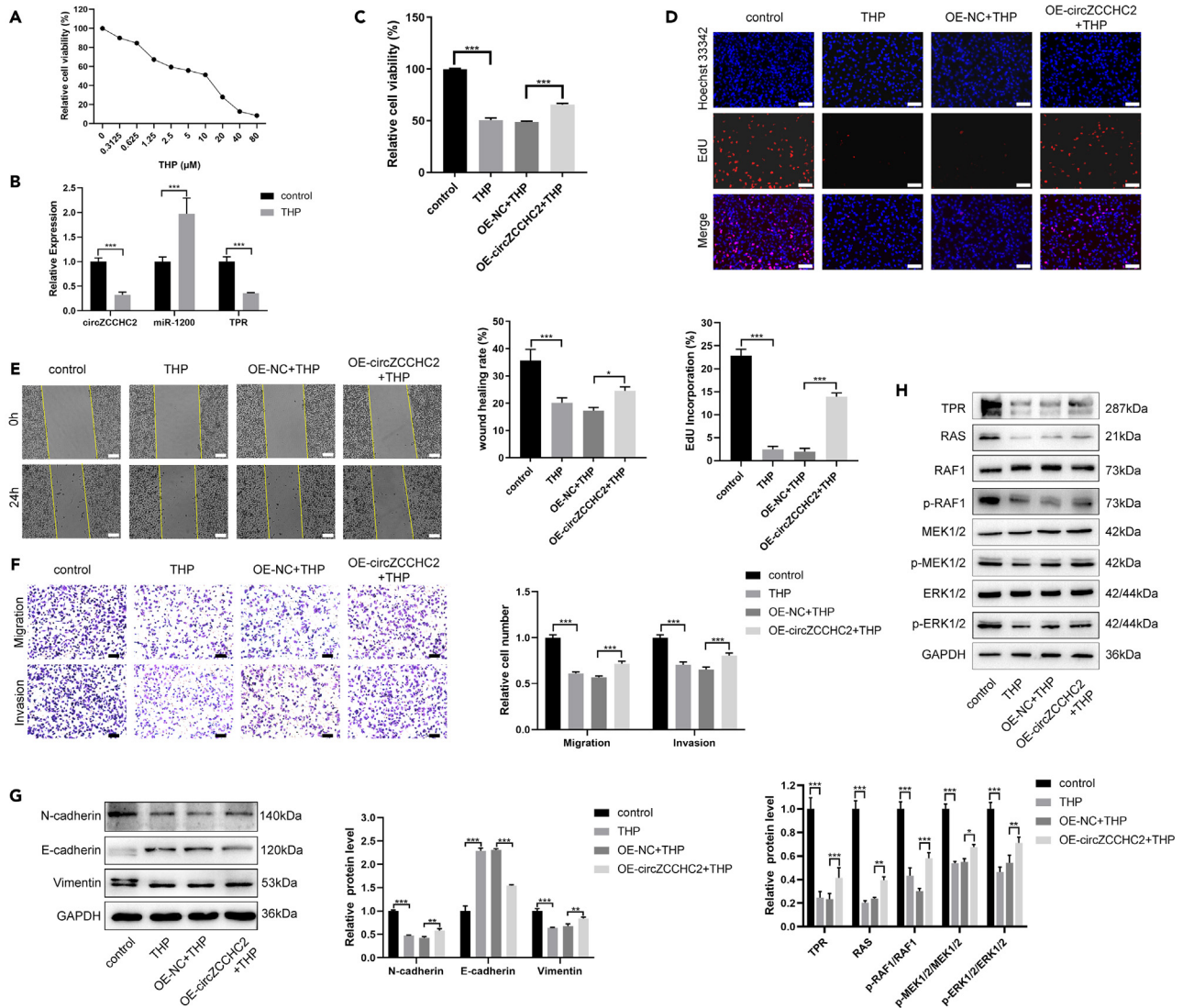


Figure 7. THP regulates circZCCHC2-mediated malignant transformation in MDA-MB-231 cells

(A) Relative viability of MDA-MB-231 cells treated with the indicated concentrations of THP for 24 h. (B) Expression changes of circZCCHC2 in TNBC cells treated with and without THP (5 μM) for 24 h. (C–H) MDA-MB-231 cells were transfected with OE-circZCCHC2 vector and treated with THP (5 μM). CCK-8 assay (C), EdU assay (D) (scale bar = 50 μm), wound-healing assay (E) (scale bar = 100 μm), Transwell assay (F) (scale bar = 20 μm), and western blotting (G) were used to analyze cell proliferation, migration, invasion, and EMT, respectively. (H) The expression levels of RAS-RAF1-MEK-ERK pathway effectors, including RAS, RAF1, p-RAF1, MEK1/2, p-MEK1/2, ERK1/2, and p-ERK1/2, were detected by western blotting. Data are presented as the mean ± SD (three independent experiments). *p < 0.05, **p < 0.01, and ***p < 0.001.

However, the development of chemotherapy resistance is an important factor leading to treatment failure and poor prognosis in BC patients. Studies have shown that the occurrence of drug resistance in cancer cells is closely related to the abnormal expression of one or more genes and the activation of related signaling pathways.^{84,85} The abnormal expression of circRNA is related to the sensitivity of BC to chemotherapy drugs.^{86,87} There have also been studies of circRNA and BC sensitivity to anthracyclines. The miR-512-3p/CDCA3 axis is responsible for promoting TNBC progression and doxorubicin resistance, which is facilitated by circUBE2D2.⁸⁸ The circRNA CREIT is downregulated in Adriamycin-resistant TNBC cells, and it is the only circRNA reported to date that can act as a protein scaffold and inhibit the PKR/eIF2α signaling axis to restore TNBC chemoresistance.⁸⁹ Additionally, circRNAs can affect sensitivity to cancer therapy through multiple mechanisms, including modulation of DNA damage repair,^{90,91} apoptosis,⁹² TME,⁹³ autophagy,⁹⁴ and glycolysis.⁹⁵ In this study, we demonstrated *in vivo* and *in vitro* that circZCCHC2 modulates the sensitivity to THP, and preliminarily validated *in vitro* that it may act through the miR-1200/TPR axis and RAS/RAG/MEK/ERK pathway. In future studies, we need to improve more experiments to further explore and explain the mechanism of circZCCHC2 affecting THP sensitivity in TNBC.

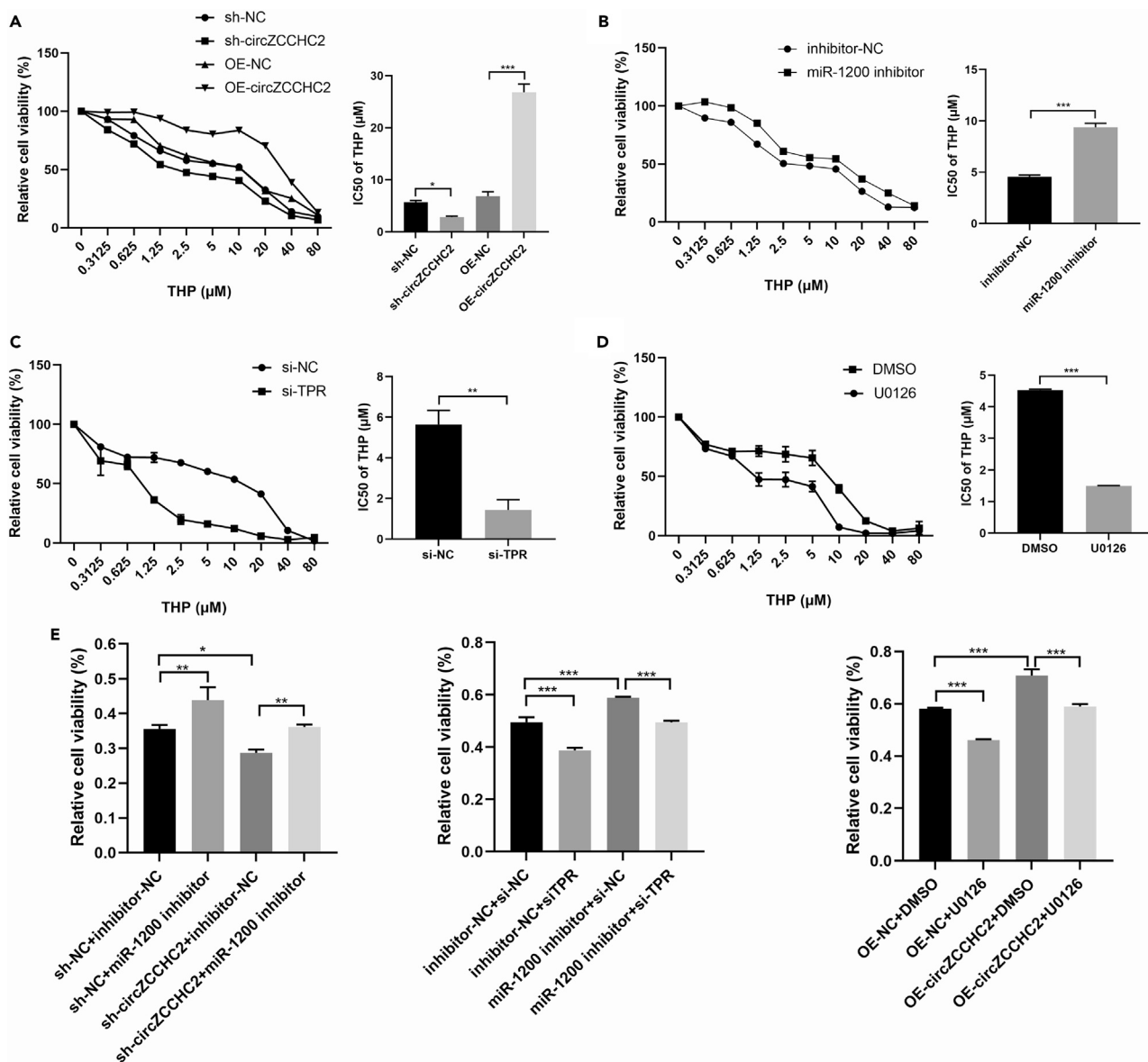


Figure 8. CircZCCHC2 affects the sensitivity of TNBC cells to pirarubicin

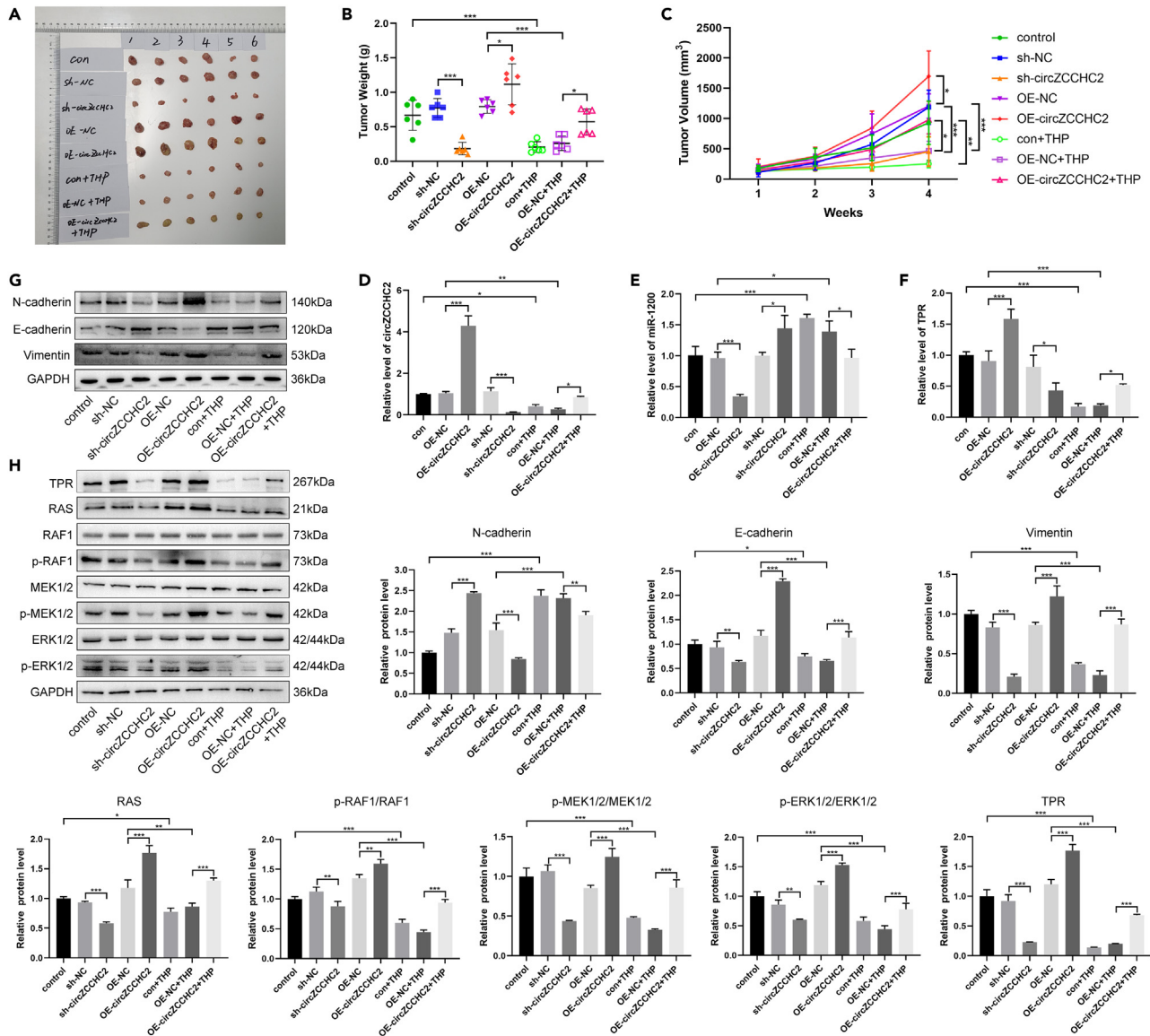
(A–D) Cell viability and IC50 of MDA-MB-231 transfected or treated with circZCCHC2 overexpression, circZCCHC2 knockdown (A), miR-1200 inhibitor (B), si-TPR (C), and U0126 (D) under THP treatment for 24 h were detected using CCK-8 assay.

(E) MDA-MB-231 cells were treated with THP (5 μM). Cell viability of MDA-MB-231 transfected or treated with circZCCHC2 overexpression, circZCCHC2 knockdown, miR-1200 inhibitor, si-TPR, and U0126 were detected using CCK-8 assay. Data are presented as the mean ± SD (three independent experiments). *p < 0.05, **p < 0.01, and ***p < 0.001.

In conclusion, we found that circZCCHC2 is overexpressed in TNBC cells, tissues, and plasma exosomes. We examined the mechanism underlying the role of circZCCHC2 in TNBC progression and demonstrated, for the first time, that circZCCHC2 modulates the effect of TPR by interacting with miR-1200. TPR activates the RAS-RAF-MEK-ERK pathway, thereby promoting the progression of TNBC. THP down-regulates circZCCHC2, and circZCCHC2 regulates THP sensitivity. The current findings may establish a theoretical framework for the use of circZCCHC2 in the treatment of TNBC.

Limitations of the study

Further exploration is necessary to elucidate the mechanism underlying the effect of THP on circZCCHC2. Furthermore, whether circZCCHC2 affects the malignant progression of BC through other mechanisms needs to be further explored. In addition, this study only provides a



preliminary analysis of how circZCCHC2 affects the TNBC sensitivity to THP, and more in-depth mechanism research needs to be improved in future studies. This study had a small clinical sample size, and larger scale studies are needed for further verification.

STAR★METHODS

Detailed methods are provided in the online version of this paper and include the following:

- KEY RESOURCES TABLE
- RESOURCE AVAILABILITY
 - Lead contact

- Materials availability
- Data and code availability
- **EXPERIMENTAL MODEL AND STUDY PARTICIPANT DETAILS**
 - Ethics approval and consent to participate
 - Human subject
 - Cell lines
 - Animals
- **METHOD DETAILS**
 - Real-time quantitative polymerase chain reaction (RT-qPCR)
 - Plasmid transfection and treatments
 - Cell proliferation assay
 - Transwell assay
 - Wound-healing assay
 - 5-Ethynyl-2'-deoxyuridine (EdU)
 - Exosome isolation and characterization
 - Western blot analysis
 - Dual luciferase reporter assay
 - Pulldown assay
 - Tumor xenograft model
- **QUANTIFICATION AND STATISTICAL ANALYSIS**
 - Statistical analysis

SUPPLEMENTAL INFORMATION

Supplemental information can be found online at <https://doi.org/10.1016/j.isci.2024.109057>.

ACKNOWLEDGMENTS

We thank International Science Editing (<http://www.internationalscienceediting.com>) for editing this manuscript.

AUTHOR CONTRIBUTIONS

F.Z.-conceived and designed the experiments, performed data analysis and wrote the manuscript. F.Z., D.W. and S.Q.-performed the experiments. L.R.-conceived and designed the experiments. D.W., S.X., S.Q., and L.L. participated in the preparation of reagents, materials and analysis tools. Z.F.-supervised the manuscript. All authors read and approved the final manuscript.

DECLARATION OF INTERESTS

The authors declare no competing interests.

Received: September 24, 2023

Revised: December 11, 2023

Accepted: January 24, 2024

Published: January 26, 2024

REFERENCES

1. Ferlay, J., Colombet, M., Soerjomataram, I., Parkin, D.M., Piñeros, M., Znaor, A., and Bray, F. (2021). Cancer statistics for the year 2020: An overview. *Int. J. Cancer* 149, 778–789. <https://doi.org/10.1002/ijc.33588>.
2. Fahad Ullah, M. (2019). Breast Cancer: Current Perspectives on the Disease Status. *Adv. Exp. Med. Biol.* 1152, 51–64. https://doi.org/10.1007/978-3-030-20301-6_4.
3. Garrido-Castro, A.C., Lin, N.U., and Polyak, K. (2019). Insights into Molecular Classifications of Triple-Negative Breast Cancer: Improving Patient Selection for Treatment. *Cancer Discov.* 9, 176–198. <https://doi.org/10.1158/2159-8290.Cd-18-1177>.
4. Liu, Z., Zhou, Y., Liang, G., Ling, Y., Tan, W., Tan, L., Andrews, R., Zhong, W., Zhang, X., Song, E., and Gong, C. (2019). Circular RNA hsa_circ_001783 regulates breast cancer progression via sponging miR-200c-3p. *Cell Death Dis.* 10, 55. <https://doi.org/10.1038/s41419-018-1287-1>.
5. Cao, L., Wang, M., Dong, Y., Xu, B., Chen, J., Ding, Y., Qiu, S., Li, L., Karamfilova Zaharieva, E., Zhou, X., and Xu, Y. (2020). Circular RNA circRNF20 promotes breast cancer tumorigenesis and Warburg effect through miR-487a/HIF-1 α /HK2. *Cell Death Dis.* 11, 145. <https://doi.org/10.1038/s41419-020-2336-0>.
6. Zeng, Y., Du, W., Huang, Z., Wu, S., Ou, X., Zhang, J., Peng, C., Sun, X., and Tang, H. (2023). Hsa_circ_0060467 promotes breast cancer liver metastasis by complexing with eIF4A3 and sponging miR-1205. *Cell Death Dis.* 9, 153. <https://doi.org/10.1038/s41420-023-01448-4>.
7. Liu, P., Wang, Z., Ou, X., Wu, P., Zhang, Y., Wu, S., Xiao, X., Li, Y., Ye, F., and Tang, H. (2022). The FUS/circEZH2/KLF5/feedback loop contributes to CXCR4-induced liver metastasis of breast cancer by enhancing epithelial-mesenchymal transition. *Mol. Cancer* 21, 198. <https://doi.org/10.1186/s12943-022-01653-2>.
8. Liu, Y., Chen, S., Zong, Z.H., Guan, X., and Zhao, Y. (2020). CircRNA WHSC1 targets the miR-646/NPM1 pathway to promote the development of endometrial cancer. *J. Cell Mol. Med.* 24, 6898–6907. <https://doi.org/10.1111/jcmm.15346>.
9. Long, F., Li, L., Xie, C., Ma, M., Wu, Z., Lu, Z., Liu, B., Yang, M., Zhang, F., Ning, Z., et al.

- (2023). Intergenic CircRNA Circ_0007379 Inhibits Colorectal Cancer Progression by Modulating miR-320a Biogenesis in a KSRP-Dependent Manner. *Int. J. Biol. Sci.* 19, 3781–3803. <https://doi.org/10.7150/ijbs.85063>.
10. Chen, G., Han, P., Zhang, Q., Li, M., Song, T., Chen, Z., Zhao, Y., Yin, D., and Lv, J. (2023). Circ_LDLR promotes the progression of papillary thyroid carcinoma by regulating miR-1294/HMGB3 axis. *J. Biochem. Mol. Toxicol.* 37, e23498. <https://doi.org/10.1002/jbt.23498>.
 11. Barghouthi, N., Turner, J., and Perini, J. (2018). Breast Cancer Development in a Transgender Male Receiving Testosterone Therapy. *Case Rep. Endocrinol.* 2018, 3652602. <https://doi.org/10.1155/2018/3652602>.
 12. Legnini, I., Di Timoteo, G., Rossi, F., Morlando, M., Briganti, F., Sthandier, O., Fatica, A., Santini, T., Andronache, A., Wade, M., et al. (2017). Circ-ZNF609 Is a Circular RNA that Can Be Translated and Functions in Myogenesis. *Mol. Cell* 66, 22–37. <https://doi.org/10.1016/j.molcel.2017.02.017>.
 13. Zhang, M., Huang, N., Yang, X., Luo, J., Yan, S., Xiao, F., Chen, W., Gao, X., Zhao, K., Zhou, H., et al. (2018). A novel protein encoded by the circular form of the SHPRH gene suppresses glioma tumorigenesis. *Oncogene* 37, 1805–1814. <https://doi.org/10.1038/s41388-017-0019-9>.
 14. Conn, V.M., Hugouvieux, V., Nayak, A., Conos, S.A., Capovilla, G., Cildir, G., Jourdain, A., Tergaonkar, V., Schmid, M., Zubieta, C., and Conn, S.J. (2017). A circRNA from SEPALLATA3 regulates splicing of its cognate mRNA through R-loop formation. *Nat. Plants* 3, 17053. <https://doi.org/10.1038/nplants.2017.53>.
 15. Zang, J., Lu, D., and Xu, A. (2020). The interaction of circRNAs and RNA binding proteins: An important part of circRNA maintenance and function. *J. Neurosci. Res.* 98, 87–97. <https://doi.org/10.1002/jnr.24356>.
 16. Ma, N., Pan, J., Wen, Y., Wu, Q., Yu, B., Chen, X., Wan, J., and Zhang, W. (2021). circTulp4 functions in Alzheimer's disease pathogenesis by regulating its parental gene. *Mol. Ther.* 29, 2167–2181. <https://doi.org/10.1016/j.yjth.2021.02.008>.
 17. Lin, G., Li, J., Chen, K., Wang, A., and Guo, C. (2022). Circ_0000854 regulates the progression of hepatocellular carcinoma through miR-1294/IRGQ axis. *Clin. Immunol.* 238, 109007. <https://doi.org/10.1016/j.clim.2022.109007>.
 18. Huang, T., Song, C., Zheng, L., Xia, L., Li, Y., and Zhou, Y. (2019). The roles of extracellular vesicles in gastric cancer development, microenvironment, anti-cancer drug resistance, and therapy. *Mol. Cancer* 18, 62. <https://doi.org/10.1186/s12943-019-0967-5>.
 19. Ding, L., Zheng, Q., Lin, Y., Wang, R., Wang, H., Luo, W., Lu, Z., Xie, H., Ren, L., Lu, H., et al. (2023). Exosome-derived circTFDP2 promotes prostate cancer progression by preventing PARP1 from caspase-3-dependent cleavage. *Clin. Transl. Med.* 13, e1156. <https://doi.org/10.1002/ctm2.1156>.
 20. Lin, J., Wang, X., Zhai, S., Shi, M., Peng, C., Deng, X., Fu, D., Wang, J., and Shen, B. (2022). Hypoxia-induced exosomal circPDK1 promotes pancreatic cancer glycolysis via c-myc activation by modulating miR-628-3p/BPTF axis and degrading BIN1. *J. Hematol. Oncol.* 15, 128. <https://doi.org/10.1186/s13045-022-01348-7>.
 21. Zhou, B., Mo, Z., Lai, G., Chen, X., Li, R., Wu, R., Zhu, J., and Zheng, F. (2023). Targeting tumor exosomal circular RNA cSERPINE2 suppresses breast cancer progression by modulating MALT1-NF-. *J. Exp. Clin. Cancer Res.* 42, 48. <https://doi.org/10.1186/s13046-023-02620-5>.
 22. Chen, S., Chen, Z., Li, Z., Li, S., Wen, Z., Cao, L., Chen, Y., Xue, P., Li, H., and Zhang, D. (2022). Tumor-associated macrophages promote cholangiocarcinoma progression via exosomal Circ_0020256. *Cell Death Dis.* 13, 94. <https://doi.org/10.1038/s41419-022-04534-0>.
 23. Qian, Y., Li, Y., Xu, L., Chen, K., Liu, N., Yang, X., Lv, Q., Li, R., Zhou, C., Xu, Z., et al. (2022). Tumor Cell-Derived Exosomal circ-PRKCI Promotes Proliferation of Renal Cell Carcinoma via Regulating miR-545-3p/CCND1 Axis. *Cancers* 15, 123. <https://doi.org/10.3390/cancers15010123>.
 24. Ambrosini, G., Rai, A.J., Carvajal, R.D., and Schwartz, G.K. (2022). Uveal Melanoma Exosomes Induce a Prometastatic Microenvironment through Macrophage Migration Inhibitory Factor. *Mol. Cancer Res.* 20, 661–669. <https://doi.org/10.1158/1541-7786.Mcr-21-0526>.
 25. Zhao, K., Cheng, X., Ye, Z., Li, Y., Peng, W., Wu, Y., and Xing, C. (2021). Exosome-Mediated Transfer of circ_0000338 Enhances 5-Fluorouracil Resistance in Colorectal Cancer through Regulating MicroRNA 217 (miR-217) and miR-485-3p. *Mol. Cell Biol.* 41, e00517-20. <https://doi.org/10.1128/mcb.00517-20>.
 26. Pan, B., Qin, J., Liu, X., He, B., Wang, X., Pan, Y., Sun, H., Xu, T., Xu, M., Chen, X., et al. (2019). Identification of Serum Exosomal hsa-circ-0004771 as a Novel Diagnostic Biomarker of Colorectal Cancer. *Front. Genet.* 10, 1096. <https://doi.org/10.3389/fgene.2019.01096>.
 27. Li, J., Ma, M., Yang, X., Zhang, M., Luo, J., Zhou, H., Huang, N., Xiao, F., Lai, B., Lv, W., and Zhang, N. (2020). Circular HER2 RNA positive triple negative breast cancer is sensitive to Pertuzumab. *Mol. Cancer* 19, 142. <https://doi.org/10.1186/s12943-020-01259-6>.
 28. Ma, J., Wang, F., Chen, C., Ji, J., Huang, P., Wei, D., Zhang, Y., and Ren, L. (2023). Identification of prognostic genes signature and construction of ceRNA network in pirarubicin treatment of triple-negative breast cancer. *Breast Cancer* 30, 379–392. <https://doi.org/10.1007/s12282-023-01433-w>.
 29. Peng, D., Luo, L., Zhang, X., Wei, C., Zhang, Z., and Han, L. (2022). CircRNA: An emerging star in the progression of glioma. *Biomedicine & pharmacotherapy = Biomedicine & pharmacotherapie* 151, 113150. <https://doi.org/10.1016/j.biopha.2022.113150>.
 30. De Palma, F.D.E., Salvatore, F., Pol, J.G., Kroemer, G., and Maiuri, M.C. (2022). Circular RNAs as Potential Biomarkers in Breast Cancer. *Biomedicines* 10, 725. <https://doi.org/10.3390/biomedicines10030725>.
 31. Li, Y., Wang, Z., Su, P., Liang, Y., Li, Z., Zhang, H., Song, X., Han, D., Wang, X., Liu, Y., et al. (2022). circ-EIF6 encodes EIF6-224aa to promote TNBC progression via stabilizing MYH9 and activating the Wnt/beta-catenin pathway. *Mol. Ther.* 30, 415–430. <https://doi.org/10.1016/j.yjth.2021.08.026>.
 32. Li, J., Gao, X., Zhang, Z., Lai, Y., Lin, X., Lin, B., Ma, M., Liang, X., Li, X., Lv, W., et al. (2021). CircCD44 plays oncogenic roles in triple-negative breast cancer by modulating the miR-502-5p/KRAS and IGF2BP2/Myc axes. *Mol. Cancer* 20, 138. <https://doi.org/10.1186/s12943-021-01444-1>.
 33. Zheng, X., Huang, M., Xing, L., Yang, R., Wang, X., Jiang, R., Zhang, L., and Chen, J. (2020). The circRNA circSEPT9 mediated by E2F1 and EIF4A3 facilitates the carcinogenesis and development of triple-negative breast cancer. *Mol. Cancer* 19, 173. <https://doi.org/10.1186/s12943-020-01183-9>.
 34. Xing, Z., Wang, R., Wang, X., Liu, J., Zhang, M., Feng, K., and Wang, X. (2021). CircRNA circ-PDCD11 promotes triple-negative breast cancer progression via enhancing aerobic glycolysis. *Cell Death Dis.* 7, 218. <https://doi.org/10.1038/s41420-021-00604-y>.
 35. Qi, X., Lin, Y., Chen, J., and Shen, B. (2020). Decoding competing endogenous RNA networks for cancer biomarker discovery. *Briefings Bioinf.* 21, 441–457. <https://doi.org/10.1093/bib/bbz006>.
 36. Piwecka, M., Glažar, P., Hernandez-Miranda, L.R., Memczak, S., Wolf, S.A., Rybak-Wolf, A., Filipchyk, A., Klironomos, F., Cerda-Jara, C.A., Fenske, P., et al. (2017). Loss of a mammalian circular RNA locus causes miRNA deregulation and affects brain function. *Science* 357. <https://doi.org/10.1126/science.aam8526>.
 37. Xue, X.L., Zhao, S., Xu, M.C., Li, Y., Liu, W.F., and Qin, H.Z. (2023). Circular RNA_0000326 accelerates breast cancer development via modulation of the miR-9-3p/YAP1 axis. *Neoplasma* 70, 430–442. https://doi.org/10.4149/neo_2023_220904N894.
 38. Song, R., Guo, P., Ren, X., Zhou, L., Li, P., Rahman, N.A., Wolczyński, S., Li, X., Zhang, Y., Liu, M., et al. (2023). A novel polypeptide CAPG-171aa encoded by circCAPG plays a critical role in triple-negative breast cancer. *Mol. Cancer* 22, 104. <https://doi.org/10.1186/s12943-023-01806-x>.
 39. Lu, Q., Sun, H., Yu, Q., and Tang, D. (2023). Circ_PRDM5/miR-25-3p/ANKRD46 axis is associated with cell malignant behaviors in subjects with breast cancer evaluated by ultrasound. *J. Biochem. Mol. Toxicol.* 37, e23469. <https://doi.org/10.1002/jbt.23469>.
 40. Wang, Z., Li, Y., Yang, J., Liang, Y., Wang, X., Zhang, N., Kong, X., Chen, B., Wang, L., Zhao, W., and Yang, Q. (2022). Circ-TRIO promotes TNBC progression by regulating the miR-432-5p/CCDC58 axis. *Cell Death Dis.* 13, 776. <https://doi.org/10.1038/s41419-022-05216-7>.
 41. He, R., Liu, P., Xie, X., Zhou, Y., Liao, Q., Xiong, W., Li, X., Li, G., Zeng, Z., and Tang, H. (2017). circGFRA1 and GFRA1 act as ceRNAs in triple negative breast cancer by regulating miR-34a. *J. Exp. Clin. Cancer Res.* 36, 145. <https://doi.org/10.1186/s13046-017-0614-1>.
 42. Li, S., Pei, Y., Wang, W., Liu, F., Zheng, K., and Zhang, X. (2019). Circular RNA 0001785 regulates the pathogenesis of osteosarcoma as a ceRNA by sponging miR-1200 to upregulate HOXB2. *Cell Cycle* 18, 1281–1291. <https://doi.org/10.1080/15384101.2019.1618127>.
 43. Luo, Y., and Yao, Q. (2022). Circ_0085315 promotes cell proliferation, invasion, and migration in colon cancer through miR-1200/MAP3K1 signaling pathway. *Cell Cycle* 21, 1194–1211. <https://doi.org/10.1080/15384101.2022.2044137>.
 44. Dewi, F.R.P., Domoto, T., Hazawa, M., Kobayashi, A., Douwaki, T., Minamoto, T., and Wong, R.W. (2018). Colorectal cancer cells require glycogen synthase kinase-3β for sustaining mitosis via translocated promoter region (TPR)-dynein interaction. *Oncotarget*

- 9, 13337–13352. <https://doi.org/10.18632/oncotarget.24344>.
45. Hoelz, A., Glavy, J.S., and Beck, M. (2016). Toward the atomic structure of the nuclear pore complex: when top down meets bottom up. *Nat. Struct. Mol. Biol.* 23, 624–630. <https://doi.org/10.1038/nsmb.3244>.
 46. Dewi, F.R.P., Jiapaer, S., Kobayashi, A., Hazawa, M., Ikiptikawati, D.K., Hartono, Sabit, H., Nakada, M., and Wong, R.W. (2021). Nucleoporin TPR (translocated promoter region, nuclear basket protein) upregulation alters MTOR-HSF1 trails and suppresses autophagy induction in ependymoma. *Autophagy* 17, 1001–1012. <https://doi.org/10.1080/15548627.2020.1741318>.
 47. Kobayashi, A., Hashizume, C., Dowaki, T., and Wong, R.W. (2015). Therapeutic potential of mitotic interaction between the nucleoporin Tpr and aurora kinase A. *Cell Cycle* 14, 1447–1458. <https://doi.org/10.1080/15384101.2015.1021518>.
 48. Nakano, H., Funasaka, T., Hashizume, C., and Wong, R.W. (2010). Nucleoporin translocated promoter region (Tpr) associates with dynein complex, preventing chromosome lagging formation during mitosis. *J. Biol. Chem.* 285, 10841–10849. <https://doi.org/10.1074/jbc.M110.105890>.
 49. Yuan, K., Lan, J., Xu, L., Feng, X., Liao, H., Xie, K., Wu, H., and Zeng, Y. (2022). Long noncoding RNA TLNC1 promotes the growth and metastasis of liver cancer via inhibition of p53 signaling. *Mol. Cancer* 21, 105. <https://doi.org/10.1186/s12943-022-01578-w>.
 50. Chen, M., Long, Q., Borrie, M.S., Sun, H., Zhang, C., Yang, H., Shi, D., Gartenberg, M.R., and Deng, W. (2021). Nucleoporin TPR promotes tRNA nuclear export and protein synthesis in lung cancer cells. *PLoS Genet.* 17, e1009899. <https://doi.org/10.1371/journal.pgen.1009899>.
 51. Du, C., Zhang, J.L., Wang, Y., Zhang, Y.Y., Zhang, J.H., Zhang, L.F., and Li, J.R. (2020). The Long Non-coding RNA LINC01705 Regulates the Development of Breast Cancer by Sponging miR-186-5p to Mediate TPR Expression as a Competitive Endogenous RNA. *Front. Genet.* 11, 779. <https://doi.org/10.3389/fgene.2020.00779>.
 52. Ullah, R., Yin, Q., Snell, A.H., and Wan, L. (2022). RAF-MEK-ERK pathway in cancer evolution and treatment. *Semin. Cancer Biol.* 85, 123–154. <https://doi.org/10.1016/j.semcancer.2021.05.010>.
 53. McCubrey, J.A., Steelman, L.S., Chappell, W.H., Abrams, S.L., Wong, E.W.T., Chang, F., Lehmann, B., Terrian, D.M., Milella, M., Tafuri, A., et al. (2007). Roles of the Raf/MEK/ERK pathway in cell growth, malignant transformation and drug resistance. *Biochim. Biophys. Acta* 1773, 1263–1284. <https://doi.org/10.1016/j.bbamcr.2006.10.001>.
 54. Mandal, R., Becker, S., and Strebhardt, K. (2016). Stamping out RAF and MEK1/2 to inhibit the ERK1/2 pathway: an emerging threat to anticancer therapy. *Oncogene* 35, 2547–2561. <https://doi.org/10.1038/onc.2015.329>.
 55. Dhillon, A.S., Hagan, S., Rath, O., and Kolch, W. (2007). MAP kinase signalling pathways in cancer. *Oncogene* 26, 3279–3290. <https://doi.org/10.1038/sj.onc.1210421>.
 56. Ouyang, L., Chen, Y., Wang, X.Y., Lu, R.F., Zhang, S.Y., Tian, M., Xie, T., Liu, B., and He, G. (2014). Polygonatum odoratum lectin induces apoptosis and autophagy via targeting EGFR-mediated Ras-Raf-MEK-ERK pathway in human MCF-7 breast cancer cells. *Phytomedicine* 21, 1658–1665. <https://doi.org/10.1016/j.phymed.2014.08.002>.
 57. Yang, X., Shang, P., Yu, B., Jin, Q., Liao, J., Wang, L., Ji, J., and Guo, X. (2021). Combination therapy with miR34a and doxorubicin synergistically inhibits Dox-resistant breast cancer progression via down-regulation of Snail through suppressing Notch/NF-κB and RAS/RAF/MEK/ERK signaling pathway. *Acta Pharm. Sin. B* 11, 2819–2834. <https://doi.org/10.1016/j.apsb.2021.06.003>.
 58. Dong, Q., Yang, B., Han, J.G., Zhang, M.M., Liu, W., Zhang, X., Yu, H.L., Liu, Z.G., Zhang, S.H., Li, T., et al. (2019). A novel hydrogen sulfide-releasing donor, HA-ADT, suppresses the growth of human breast cancer cells through inhibiting the PI3K/AKT/mTOR and Ras/Raf/MEK/ERK signaling pathways. *Cancer Lett.* 455, 60–72. <https://doi.org/10.1016/j.canlet.2019.04.031>.
 59. Lee, J., Lim, B., Pearson, T., Choi, K., Fuson, J.A., Bartholomeusz, C., Paradiso, L.J., Myers, T., Tripathy, D., and Ueno, N.T. (2019). Anti-tumor and anti-metastasis efficacy of E6201, a MEK1 inhibitor, in preclinical models of triple-negative breast cancer. *Breast Cancer Res. Treat.* 175, 339–351. <https://doi.org/10.1007/s10549-019-05166-3>.
 60. Poursani, E.M., Mercatelli, D., Raninga, P., Bell, J.L., Saletta, F., Kohane, F.V., Neumann, D.P., Zheng, Y., Rouaen, J.R.C., Jue, T.R., et al. (2023). Copper chelation suppresses epithelial-mesenchymal transition by inhibition of canonical and non-canonical TGF-β signaling pathways in cancer. *Cell Biosci.* 13, 132. <https://doi.org/10.1186/s13578-023-01083-7>.
 61. Humphries, B.A., Cutter, A.C., Buschhaus, J.M., Chen, Y.C., Qyli, T., Palagama, D.S.W., Eckley, S., Robison, T.H., Bevoor, A., Chiang, B., et al. (2020). Enhanced mitochondrial fission suppresses signaling and metastasis in triple-negative breast cancer. *Breast Cancer Res.* 22, 60. <https://doi.org/10.1186/s13058-020-01301-x>.
 62. Hegmans, J.P.J.J., Gerber, P.J., and Lambrecht, B.N. (2008). Exosomes. *Methods Mol. Biol.* 484, 97–109. https://doi.org/10.1007/978-1-59745-398-1_7.
 63. Andre, F., Scharzt, N.E.C., Movassagh, M., Flament, C., Pautier, P., Morice, P., Pomel, C., Lhomme, C., Escudier, B., Le Chevalier, T., et al. (2002). Malignant effusions and immunogenic tumour-derived exosomes. *Lancet* 360, 295–305. [https://doi.org/10.1016/s0140-6736\(02\)09552-1](https://doi.org/10.1016/s0140-6736(02)09552-1).
 64. Caby, M.P., Lankar, D., Vincendeau-Scherrer, C., Raposo, G., and Bonnerot, C. (2005). Exosomal-like vesicles are present in human blood plasma. *Int. Immunol.* 17, 879–887. <https://doi.org/10.1093/intimm/dxh267>.
 65. Pisitkun, T., Shen, R.F., and Knepper, M.A. (2004). Identification and proteomic profiling of exosomes in human urine. *Proc. Natl. Acad. Sci. USA* 101, 13368–13373. <https://doi.org/10.1073/pnas.0403453101>.
 66. Admyre, C., Johansson, S.M., Qazi, K.R., Filén, J.J., Laheesmaa, R., Norman, M., Neve, E.P.A., Schevnius, A., and Gabrielsson, S. (2007). Exosomes with immune modulatory features are present in human breast milk. *J. Immunol.* 179, 1969–1978. <https://doi.org/10.4049/jimmunol.179.3.1969>.
 67. Romano, E., Netti, P.A., and Torino, E. (2021). A High Throughput Approach Based on Dynamic High Pressure for the Encapsulation of Active Compounds in Exosomes for Precision Medicine. *Int. J. Mol. Sci.* 22, 9896. <https://doi.org/10.3390/ijms22189896>.
 68. Ghafouri-Fard, S., Niazi, V., Hussen, B.M., Omrani, M.D., Taheri, M., and Basiri, A. (2021). The Emerging Role of Exosomes in the Treatment of Human Disorders With a Special Focus on Mesenchymal Stem Cells-Derived Exosomes. *Front. Cell Dev. Biol.* 9, 653296. <https://doi.org/10.3389/fcell.2021.653296>.
 69. Hussen, B.M., Faraj, G.S.H., Rasul, M.F., Hidayat, H.J., Salihi, A., Baniahmad, A., Taheri, M., and Ghafouri-Frad, S. (2022). Strategies to overcome the main challenges of the use of exosomes as drug carrier for cancer therapy. *Cancer Cell Int.* 22, 323. <https://doi.org/10.1186/s12935-022-02743-3>.
 70. Liu, J., Peng, X., Liu, Y., Hao, R., Zhao, R., Zhang, L., Zhao, F., Liu, Q., Liu, Y., and Qi, Y. (2021). The Diagnostic Value of Serum Exosomal Has_circ_0000615 for Breast Cancer Patients. *Int. J. Gen. Med.* 14, 4545–4554. <https://doi.org/10.2147/ijgm.S319801>.
 71. Liu, J., Ren, L., Li, S., Li, W., Zheng, X., Yang, Y., Fu, W., Yi, J., Wang, J., and Du, G. (2021). The biology, function, and applications of exosomes in cancer. *Acta Pharm. Sin. B* 11, 2783–2797. <https://doi.org/10.1016/j.apsb.2021.01.001>.
 72. Liang, G., Liu, Z., Tan, L., Su, A.N., Jiang, W.G., and Gong, C. (2017). HIF1α-associated circDENND4C Promotes Proliferation of Breast Cancer Cells in Hypoxic Environment. *Anticancer Res.* 37, 4337–4343. <https://doi.org/10.21873/anticancer.11827>.
 73. Chen, B., Wei, W., Huang, X., Xie, X., Kong, Y., Dai, D., Yang, L., Wang, J., Tang, H., and Xie, X. (2018). circEPT11 as a Prognostic Marker and Mediator of Triple-Negative Breast Cancer Progression. *Theranostics* 8, 4003–4015. <https://doi.org/10.7150/thno.24106>.
 74. Lu, C., Shi, W., Hu, W., Zhao, Y., Zhao, X., Dong, F., Xin, Y., Peng, T., and Liu, C. (2022). Endoplasmic reticulum stress promotes breast cancer cells to release exosomes circ_0001142 and induces M2 polarization of macrophages to regulate tumor progression. *Pharmacol. Res.* 177, 106098. <https://doi.org/10.1016/j.phrs.2022.106098>.
 75. Tacar, O., Sriamornsak, P., and Dass, C.R. (2013). Doxorubicin: an update on anticancer molecular action, toxicity and novel drug delivery systems. *J. Pharm. Pharmacol.* 65, 157–170. <https://doi.org/10.1111/j.2042-7158.2012.01567.x>.
 76. Swift, L.P., Rephaeli, A., Nudelman, A., Phillips, D.R., and Cutts, S.M. (2006). Doxorubicin-DNA adducts induce a non-topoisomerase II-mediated form of cell death. *Cancer Res.* 66, 4863–4871. <https://doi.org/10.1158/0008-5472.CCR-05-3410>.
 77. Pang, B., Qiao, X., Janssen, L., Velds, A., Groothuis, T., Kerkhoven, R., Nieuwland, M., Ova, H., Rottenberg, S., van Tellingen, O., et al. (2013). Drug-induced histone eviction from open chromatin contributes to the chemotherapeutic effects of doxorubicin. *Nat. Commun.* 4, 1908. <https://doi.org/10.1038/ncomms2921>.
 78. Yang, F., Kemp, C.J., and Henikoff, S. (2013). Doxorubicin enhances nucleosome turnover around promoters. *Curr. Biol.* 23, 782–787. <https://doi.org/10.1016/j.cub.2013.03.043>.
 79. Conn, S.J., Pillman, K.A., Toubia, J., Conn, V.M., Salmanidis, M., Phillips, C.A., Roslan, S., Schreiber, A.W., Gregory, P.A., and Goodall, G.J. (2015). The RNA binding protein quaking regulates formation of circRNAs. *Cell* 160,

- 1125–1134. <https://doi.org/10.1016/j.cell.2015.02.014>.
80. Wang, R., Zhang, S., Chen, X., Li, N., Li, J., Jia, R., Pan, Y., and Liang, H. (2018). EIF4A3-induced circular RNA MMP9 (circMMP9) acts as a sponge of miR-124 and promotes glioblastoma multiforme cell tumorigenesis. *Mol. Cancer* 17, 166. <https://doi.org/10.1186/s12943-018-0911-0>.
 81. Meng, J., Chen, S., Han, J.X., Qian, B., Wang, X.R., Zhong, W.L., Qin, Y., Zhang, H., Gao, W.F., Lei, Y.Y., et al. (2018). Twist1 Regulates Vimentin through Cui2 Circular RNA to Promote EMT in Hepatocellular Carcinoma. *Cancer Res.* 78, 4150–4162. <https://doi.org/10.1158/0008-5472.Can-17-3009>.
 82. Wu, Y., Wang, Z., Han, L., Guo, Z., Yan, B., Guo, L., Zhao, H., Wei, M., Hou, N., Ye, J., et al. (2022). PRMT5 regulates RNA m6A demethylation for doxorubicin sensitivity in breast cancer. *Mol. Ther.* 30, 2603–2617. <https://doi.org/10.1016/j.ymthe.2022.03.003>.
 83. Chen, Y., Ling, Z., Cai, X., Xu, Y., Lv, Z., Man, D., Ge, J., Yu, C., Zhang, D., Zhang, Y., et al. (2022). Activation of YAP1 by N6-Methyladenosine-Modified circCPSF6 Drives Malignancy in Hepatocellular Carcinoma. *Cancer Res.* 82, 599–614. <https://doi.org/10.1158/0008-5472.Can-21-1628>.
 84. Vasan, N., Baselga, J., and Hyman, D.M. (2019). A view on drug resistance in cancer. *Nature* 575, 299–309. <https://doi.org/10.1038/s41586-019-1730-1>.
 85. Nikolaou, M., Pavlopoulou, A., Georgakilas, A.G., and Kyrodimos, E. (2018). The challenge of drug resistance in cancer treatment: a current overview. *Clin. Exp. Metastasis* 35, 309–318. <https://doi.org/10.1007/s10585-018-9903-0>.
 86. Wang, L., Zhou, Y., Jiang, L., Lu, L., Dai, T., Li, A., Chen, Y., and Zhang, L. (2021). CircWAC induces chemotherapeutic resistance in triple-negative breast cancer by targeting miR-142, upregulating WWP1 and activating the PI3K/AKT pathway. *Mol. Cancer* 20, 43. <https://doi.org/10.1186/s12943-021-01332-8>.
 87. Li, H., Xu, W., Xia, Z., Liu, W., Pan, G., Ding, J., Li, J., Wang, J., Xie, X., and Jiang, D. (2021). Hsa_circ_0000199 facilitates chemotolerance of triple-negative breast cancer by interfering with miR-206/613-led PI3K/Akt/mTOR signaling. *Aging* 13, 4522–4551. <https://doi.org/10.18632/aging.202415>.
 88. Dou, D., Ren, X., Han, M., Xu, X., Ge, X., Gu, Y., Wang, X., and Zhao, S. (2020). CircUBE2D2 (hsa_circ_0005728) promotes cell proliferation, metastasis and chemoresistance in triple-negative breast cancer by regulating miR-512-3p/CDCA3 axis. *Cancer Cell Int.* 20, 454. <https://doi.org/10.1186/s12935-020-01547-7>.
 89. Wang, X., Chen, T., Li, C., Li, W., Zhou, X., Li, Y., Luo, D., Zhang, N., Chen, B., Wang, L., et al. (2022). CircRNA-CREIT inhibits stress granule assembly and overcomes doxorubicin resistance in TNBC by destabilizing PKR. *J. Hematol. Oncol.* 15, 122. <https://doi.org/10.1186/s13045-022-01345-w>.
 90. Xu, X., Zhang, J., Tian, Y., Gao, Y., Dong, X., Chen, W., Yuan, X., Yin, W., Xu, J., Chen, K., et al. (2020). CircRNA inhibits DNA damage repair by interacting with host gene. *Mol. Cancer* 19, 128. <https://doi.org/10.1186/s12943-020-01246-x>.
 91. Erdel, F., and Rippe, K. (2011). Binding kinetics of human ISWI chromatin-remodelers to DNA repair sites elucidate their target location mechanism. *Nucleus* 2, 105–112. <https://doi.org/10.4161/nucl.2.2.15209>.
 92. Liu, Z., Gu, S., Wu, K., Li, L., Dong, C., Wang, W., and Zhou, Y. (2021). CircRNA-DOPEY2 enhances the chemosensitivity of esophageal cancer cells by inhibiting CPEB4-mediated Mcl-1 translation. *J. Exp. Clin. Cancer Res.* 40, 361. <https://doi.org/10.1186/s13046-021-02149-5>.
 93. Xu, G., Li, M., Wu, J., Qin, C., Tao, Y., and He, H. (2020). Circular RNA circNRIP1 Sponges microRNA-138-5p to Maintain Hypoxia-Induced Resistance to 5-Fluorouracil Through HIF-1 α -Dependent Glucose Metabolism in Gastric Carcinoma. *Cancer Manag. Res.* 12, 2789–2802. <https://doi.org/10.2147/cmar.S246272>.
 94. Wang, Q., Liang, D., Shen, P., Yu, Y., Yan, Y., and You, W. (2021). Hsa_circ_0092276 promotes doxorubicin resistance in breast cancer cells by regulating autophagy via miR-348/ATG7 axis. *Transl. Oncol.* 14, 101045. <https://doi.org/10.1016/j.tranon.2021.101045>.
 95. Zhao, Y., Zhong, R., Deng, C., and Zhou, Z. (2021). Circle RNA circABCB10 Modulates PFN2 to Promote Breast Cancer Progression, as Well as Aggravate Radioresistance Through Facilitating Glycolytic Metabolism Via miR-223-3p. *Cancer Biother. Radiopharm.* 36, 477–490. <https://doi.org/10.1089/cbr.2019.3389>.

STAR★METHODS

KEY RESOURCES TABLE

| REAGENT or RESOURCE | SOURCE | IDENTIFIER |
|--|--|--------------------------------|
| Antibodies | | |
| Anti-TSG101 | Affinity | Cat#DF8427; RRID: AB_2841675 |
| Anti-CD63 | Affinity | Cat#AF5117; RRID: AB_2837603 |
| Anti-N-cadherin | Affinity | Cat#AF5239; RRID: AB_2837725 |
| Anti-E-cadherin | Affinity | Cat#AF0131; RRID: AB_2833315 |
| Anti-vimentin | Affinity | Cat#AF7013; RRID: AB_2835318 |
| Anti-GAPDH | ABclonal | Cat#A19056; RRID: AB_2862549 |
| Anti-RAS | ABclonal | Cat#A19779; RRID: AB_2862751 |
| Anti-p-RAF1 | ABclonal | Cat#AP0498; RRID: AB_2771492 |
| Anti-RAF1 | ABclonal | Cat#A19638; RRID: AB_2862710 |
| Anti-p-MEK1/2 | ABclonal | Cat#AP1349 |
| Anti-MEK1/2 | ABclonal | Cat#A4868; RRID: AB_2863368 |
| Anti-p-ERK1/2 | ABclonal | Cat#AP0974; RRID: AB_2863871 |
| Biological samples | | |
| Human BC tissues, adjacent normal tissues, and blood samples | the First Hospital of Jilin University | N/A |
| Chemicals, peptides, and recombinant proteins | | |
| RPMI Medium 1640 | Procell | Cat#PM150110 |
| DMEM | Procell | Cat#PM150210 |
| Fetal bovine serum | Procell | Cat#164210 |
| DMSO | Biotopped | Cat#D6370T |
| TRIzol | Invitrogen | Cat#15596026 |
| Critical commercial assays | | |
| Hieff® Quick Exosome Isolation Kit (for Serum/Plasma) | Yeasen | Cat#41202ES30 |
| BCA Assay Kit | Yeasen | Cat#20201ES76 |
| qPCR SYBR Green Master Mix | Yeasen | Cat#11201ES08 |
| 1st Strand cDNA Synthesis SuperMix (gDNA Digester Plus) | Yeasen | Cat#11139ES60 |
| Deposited data | | |
| THP treatment chip | Ma et al. ²⁸ | PMID: 36622564 |
| RNA high-throughput sequencing | Li et al. ²⁷ | PMID: 32917240; NCBI SRP266211 |
| Experimental models: Cell lines | | |
| MDA-MB-231 | Procell | Cat#CL-0150B |
| MDA-MB-468 | Procell | Cat# CL-0290A |
| MDA-MB-436 | Chinese Academy of Sciences | N/A |
| MCF-10A | Chinese Academy of Sciences | N/A |
| MCF-7 | Chinese Academy of Sciences | N/A |
| BT-474 | Chinese Academy of Sciences | N/A |
| SK-BR3 | Chinese Academy of Sciences | N/A |
| Experimental models: Organisms | | |
| Four-week-old female BALB/c nude mice | SEPEIFU | N/A |

(Continued on next page)

Continued

| REAGENT or RESOURCE | SOURCE | IDENTIFIER |
|----------------------------------|------------------------------|------------|
| Oligonucleotides | | |
| Primer sequences | See Table S1 | N/A |
| Sequences of plasmids and siRNAs | See Table S2 | N/A |
| Software and algorithms | | |
| GraphPad Prism 9.0 | GraphPad | N/A |
| SPSS 26.0 | IBM SPSS | N/A |
| ImageJ | NIH ImageJ | N/A |

RESOURCE AVAILABILITY

Lead contact

Further information and requests for resources and reagents should be directed to and will be fulfilled by the lead contact, Zhimin Fan (fanzm@jlu.edu.cn).

Materials availability

This study did not generate new unique reagents.

Data and code availability

- Publicly accessible RNA high-throughput sequencing data was analyzed and the corresponding accession numbers are listed in the [key resources table](#).
- This paper does not report original code.
- Any additional information required to reanalyze the data reported in this paper is available from the [lead contact](#) upon request.

EXPERIMENTAL MODEL AND STUDY PARTICIPANT DETAILS

Ethics approval and consent to participate

The Ethics Review Committee of the First Hospital of Jilin University granted approval for this research (21K127-001, Nov. 25th, 2021).

The animal experiments were conducted in compliance with the regulations set by the Experimental Animal Ethics Committee of the School of Public Health at Jilin University (SY202306100, June 10th, 2023).

Human subject

BC tissues, adjacent normal tissues, and blood samples were obtained from female BC patients (including 47 TNBC patients without neoadjuvant chemotherapy (NAC), and 35 non-TNBC patients without NAC) who underwent surgical treatment between 2018 and 2019 at the First Hospital of Jilin University. The Ethics Review Committee of the First Hospital of Jilin University granted approval for this research (21K127-001, Nov. 25th, 2021). Written consent for tissues and blood samples were obtained from all patients.

Cell lines

The cell lines (MDA-MB-231, MDA-MB-468, MDA-MB-436, MCF-10A, MCF-7, BT-474, and SK-BR3) were acquired from the Cell Bank of the Chinese Academy of Sciences (Shanghai, China) and Procell (Wuhan, China). All cell lines except for MDA-MB-468 were cultured in a humidified incubator at 37°C with 5% CO₂. MDA-MB-231 and MDA-MB-436 cells were grown in DMEM supplemented with 10% FBS (Procell, Wuhan, China) and 1% penicillin/streptomycin (Yeasen, Shanghai, China). MCF-10A, BT-474, and SK-BR3 cells were grown in appropriate special complete medium. MCF-7 cells were cultured in 1640 medium enriched with 10% FBS (Procell) and 1% penicillin/streptomycin (Yeasen). MDA-MB-468 cells were cultured in L-15 medium with 10% FBS (Procell) and 1% penicillin/streptomycin (Yeasen) in a humidified incubator at 37°C without CO₂.

Animals

Four-week-old female BALB/c nude mice were acquired from SEPEIFU in Beijing, China and kept in a pathogen-free environment. The animal experiments were conducted in compliance with the regulations set by the Experimental Animal Ethics Committee of the School of Public Health at Jilin University (SY202306100, June 10th, 2023).

METHOD DETAILS

Real-time quantitative polymerase chain reaction (RT-qPCR)

The TRIzol reagent (Invitrogen, USA) was used for the extraction of total RNA from cells and tissues. A gDNA kit (TransGen Biotech, Beijing, China) was used to isolate gDNA from cells. The reverse transcription reaction utilized 1st Strand cDNA Synthesis SuperMix (gDNA Digester Plus) (Yeasen). For the RT-qPCR, 2 μ L of cDNA template was employed with qTOWER³ system (Analytik Jena, Germany) using qPCR SYBR Green Master Mix (Yeasen). GAPDH and U6 were used as internal controls to standardize the transcript levels based on the $2^{-\Delta\Delta C_t}$ method. Primers employed in this study were synthesized by Sangon Biotech from Shanghai, China (Shanghai, China) (Table S1).

Plasmid transfection and treatments

The shRNA that specifically targets circZCCHC2 was synthesized by GenePharma (Shanghai, China) and then inserted into the pcDNA3.1-GFP vector. To construct the circZCCHC2 overexpression vector, the full length human hsa_circ_0000854 was inserted into the C-1170 vector (LandM, Guangzhou, China), which contains a circular frame. Puromycin administration (Yeasen Biotech) was used to screen stable cell lines. The si-TPR, miR-1200 mimics, and miR-1200 inhibitor were purchased from GenePharma in Shanghai, China (Table S2). Transfection of plasmids, siRNA, or miRNA mimics or inhibitors was performed using GoldenTran-DR transfection reagent (Changchun Golden Transfer Science and Technology Co., Ltd., China) according to the manufacturer's instructions. MEK inhibitor U0126 (Selleck, USA) used in the study were prepared by dimethyl sulfoxide (DMSO). Final concentration used for cell experiments was 5 μ M and the treatment time lasted 24 h.

Cell proliferation assay

The TNBC cells were plated in 96-well plates and allowed to culture overnight. The wells were incubated at 37°C for 1 h after adding the CCK-8 reagent at 0, 24, 48, and 72 h. We utilized the POLARstar OPTIMA multi-detection microplate reader (BioRad, San Diego, CA, USA) to quantify the absorbance at 450 nm using.

Transwell assay

BC cells (5×10^4) were suspended in 200 μ L serum-free medium and added to the upper chamber of Transwell plates. The upper chamber was coated with Matrigel (Corning, NY 14831 USA) prior to the invasion experiment. The lower chamber was supplemented with medium (700 μ L) containing 15%FBS. Following a 24-h culture, the cells were treated with 4% paraformaldehyde for 30 min to fix them, and then stained with 0.1% crystal violet for 10 min. The cells were observed and captured utilizing a microscope, and quantified using ImageJ.

Wound-healing assay

TNBC cells were seeded into six-well plates for culture and grown to 100% monolayers. Scratches were made with 10- μ L pipette tips. Afterward, the cells were grown in a medium without serum. Images were captured at 0 and 24 h after conducting the scratches, and subsequent quantitative analyses were carried out.

5-Ethynyl-2'-deoxyuridine (EdU)

TNBC cells were placed in 96-well plates and then incubated with EdU reagent at 37°C for 2 h. Afterward, the cells were fixed with 4% paraformaldehyde for 15 min, followed by treatment with Triton-100 for 15 min and incubation at room temperature in the dark for 30 min with the reaction solution. The nuclei were stained with Hoechst 33342. The cells were eventually observed and captured using a fluorescence microscope.

Exosome isolation and characterization

Exosomes from the plasma of BC patients were isolated with the Hieff Quick Exosome Isolation Kit (for Serum/Plasma) (Yeasen) according to the manufacturer's manual. Western blotting was employed to identify the presence of positive markers, specifically CD63 (Affinity) and TSG101 (Affinity). The Malvern particle size meter was used to measure the particle size of exosomes. The morphological analysis of exosomes was conducted using transmission electron microscopy (Tecnai Spirit Biotwin) and images were observed.

Western blot analysis

Proteins were extracted from cells and tissues using RIPA buffer, and the concentration of total protein was determined using a BCA Assay Kit (Yeasen Biotech). The protein samples underwent separation using SDS-PAGE and were subsequently transferred to PVDF membranes, followed by blocking in 5% non-fat milk for 2 h. Next, the membranes were incubated with specific primary antibodies overnight at 4°C, followed by secondary antibodies for 1 h. The detection of the band signals was accomplished using an electrochemiluminescence (ECL) system. The following primary antibodies were used in this study TSG101 (Affinity), CD63 (Affinity), N-cadherin (Affinity), E-cadherin (Affinity), vimentin (Affinity), GAPDH (ABclonal), RAS (ABclonal), p-RAF1 (ABclonal), RAF1 (ABclonal), p-MEK1/2 (ABclonal), MEK1/2 (ABclonal), p-ERK1/2 (ABclonal), ERK1/2 (ABclonal), and TPR (Abcam).

Dual luciferase reporter assay

CircZCCHC2 or TPR 3'UTR sequences containing the wild-type- and mutant miR-1200-binding sites were synthesized and inserted into dual luciferase reporter plasmids (Promega, USA) that included the psiCheck2 promoter. BC cells were co-transfected with the miR-1299 mimics or control mimics. Luciferase activity was measured using the Dual-Luciferase Reporter Assay System (Promega) after 48 h.

Pulldown assay

MDA-MB-231 and MDA-MB-436 cells were transfected with biotinylated miR-1200 probe and negative control probe, which were designed by Ibsbio (Shanghai, China). The cells were harvested after 48 h, and then magnetic bead sealing, cell lysis, and magnetic bead hybridization incubation steps were carried out according to the instructions provided by the manufacturer of the miRNA pulldown kit (BersinBio, Guangzhou, China). The RNA complexes bound to the beads were eluted and extracted for RT-qPCR analysis to evaluate the abundance of circZCCHC2 and TPR.

Tumor xenograft model

Stable cell lines (1×10^7) were subcutaneously injected into each mouse, and the tumor volume were monitored and recorded regularly according to the formula: volume = (width² × length)/2. Four weeks after injection, the mice were sacrificed. For *in vivo* drug experiments, 1 week after cell injection, THP or 5% glucose solution was administered by tail vein injection at a dose of 5 mg/kg.

QUANTIFICATION AND STATISTICAL ANALYSIS

Statistical analysis

Each experiment was repeated at least three times. GraphPad Prism 9.0 and SPSS 26.0 software were used for statistical analysis, and $p < 0.05$ was considered statistically significant. The mean \pm SD was used to express the experimental data. The two-sided Student's *t* test was used to evaluate differences between two groups, and one-way analysis of variance (ANOVA) was used to evaluate differences among multiple groups. The association of circZCCHC2 with miR-1200, TPR, and clinicopathological characteristics was determined by the χ^2 test and Fisher's exact test, and the correlation was assessed by Pearson's correlation analysis. To assess the diagnostic value of circZCCHC2 for BC, a receiver operating characteristic (ROC) curve was generated. * $p < 0.05$, ** $p < 0.01$, *** $p < 0.001$, and ns: not significant.